Soil moisture and vegetation dynamics in Southern Great Plains Grasslands

By

SONISA SHARMA

Bachelor of Science in Agriculture
Tribhuvan University
Rampur, Chitwan
2008

Master of Science in Natural Resources
University of Nebraska- Lincoln
Lincoln, Nebraska
2013

Submitted to the Faculty of the
Graduate College of the
Oklahoma State University
in partial fulfillment of
the requirements for
the Degree of
DOCTOR OF PHILOSOPHY
July, 2017

SOIL MOISTURE AND VEGETATION DYNAMICS

IN SOUTHERN GREAT PLAINS GRASSLANDS

Dissertation Approved:

Dr. Tyson Ochsner

Dissertation Adviser

Dr. Phillip Alderman

Dr. Alex Rocateli

Dr. Samuel. D. Fuelendorf

ACKNOWLEDGEMENTS

I would like to thank a number of people for their input and assistance in this endeavor. I could not have accomplished as much as I did without them, and they have all played an important role in my studies. I would most like to thank my adviser, Dr. Tyson Ochsner, who not only provided valuable insight throughout my study, but also gave me the opportunity to pursue graduate level education. I would also like to thank my committee members, Dr. Phillip Alderman, Dr. Alex Rocateli, and Dr. Samuel D. Fuhlendorf. Their input was certainly valued and ultimately made for a superior finished product.

I am very much thankful to Dr. David Engle for mentoring me in two of my dissertation chapters. Special thanks to Drs. JD Carlson and Dirac Twidwell for their role in providing the data. Very special thanks to Andres Patrignani, Lei Feng, Geano Dong, Destiny Barker, Philip Pope, Thomas Spadea, and Erik Krueger for their valuable inputs in data collection, Matlab code and feedback on the manuscripts. A very special thanks to my husband Kundan Dhakal for all the help, and for always being by my side helping, encouraging and supporting me in all-important decisions to be made. A special thanks to my son Nirvik Dhakal for teaching me the value of patience in life.

Finally, I would like to thank my family, especially my Parents Mr. Krishna Prasad Tiwari and Mrs. Ganga Devi Tiwari, my brother Nischal Tiwari and my mother-in law Mrs. Tara Dhakal for their continuous love and support. I must not overlook the rest of the faculty, staff, and fellow graduate students in the Department of Plant and Soil Sciences, as I have certainly enjoyed working with all of them. I would also like to thank fellow graduate students Yohannes Yiman, Briana Wyatt, Jordan Beehler, and Xuili Xin. All of them have all helped me in one way or another, especially by giving me advice and listening to me if I had problems or questions. They have also made the work much more enjoyable, and I'm not sure if it is possible to find more dedicated and enthusiastic students

Name: SONISA SHARMA

Date of Degree: JULY, 2017

Title of Study: SOIL MOISTURE AND VEGETATION DYNAMICS IN SOUTHERN GREAT PLAINS GRASSLANDS

Major Field: Soil Science

Abstract:

This dissertation consists of three research projects aimed at better understanding grassland vegetation dynamics under drought and predicting vegetation dynamics using soil moisture and other vegetation parameters. The objective of the first project was to develop nondestructive methods of estimating aboveground biomass and fuel moisture content in our study area. We calibrated and validated both stepwise multiple linear regression (SMLR) and artificial neural network (ANN) models for Above-Ground Biomass (AGB) and Fuel Moisture Content (FMC) using data collected in grasslands near Stillwater, OK, USA. Our study spanned two growing seasons and nine patches located within three pastures under patch burn management. Day of year, canopy height, Normalized Difference Vegetation Index (NDVI), and percent reflectance at five spectral bands were candidate input variables for the models. For AGB, the ANN and SMLR models performed similarly (RMSE = 110 g m^{-2} versus 114 g m^{-2}). For FMC, the ANN models proved better than SMLR models (RMSE = 23.3% versus RMSE = 27.7%). Given the large variability in the underlying datasets, these models may prove useful for nondestructive estimation of AGB and FMC in other similar grassland environments. The objective of the second study was to quantify the temporal dynamics of LFMC (live FMC), live fuel mass, dead fuel mass, and soil moisture expressed as fraction of available water capacity (FAW), and to describe how LFMC and live to dead fuel transition are related to FAW. LFMC exhibited a nonlinear, threshold-type relationship with FAW, with LFMC being insensitive to FAW at FAW levels above approximately 0.56 and positively related to FAW below that threshold. Live to dead fuel transitions occurred around a FAW value of approximately 0.34, with the rate of transition increasing linearly as FAW dropped below that threshold. In light of these findings and the increasing availability of soil moisture data, a logical next step would be to develop ways to incorporate soil moisture information into dynamic fuel bed models for improved fire danger assessments and enhanced wildfire preparedness. The objective of the third study was to evaluate the CROPGRO perennial forage model for simulating forage production and soil moisture in tallgrass prairie using the previously calibrated plant parameters from the literature. The uncalibrated forage model was not effective in estimating live mass but it was reasonably accurate in estimating the soil moisture. In light of this finding, the next step would be calibrating the model's plant parameters from the observed live mass data to allow improved prediction accuracy from the model.

TABLE OF CONTENTS

LIST OF TABLES

CHAPTER II

Table

CHAPTER IV

Table

LIST OF FIGURES

CHAPTER II

Figure

CHAPTER III

Figure

CHAPTER IV

Figure

CHAPTER I

GENERAL INTRODUCTION

Grasslands and grazing systems are essential to agricultural communities in the United States Southern Great Plains (SGP) and in similar climatic regions around the world. In the SGP states of Kansas, Oklahoma, and Texas, cattle and calf production added about $100 billion to the economy in 2011. Additionally, hay production in 2011 was 10 million Mg which added another $1 billion to the region's economy. The SGP contains 55 million ha of total pasture area, including permanent pasture, and cropland used for pasture and pasture woodland. Of that 55 million ha, 9 million ha of pasture were located in Oklahoma in 2011 (NASS-USDA, 2012). Wise management of these grasslands and grazing systems is necessary not only for economic reasons, but also to conserve soil, protect water quality, and maintain ecosystem services (Belsky et al., 1999; Follett and Reed, 2010; Worrall et al., 2007). However, grassland management in the SGP is challenging because the variable climate creates large uncertainties regarding the vegetation productivity both within and between seasons.

Extreme temperature and erratic rainfall patterns are characteristic features of the climate in the drought-prone SGP (Basara et al., 2013). For example, in 2011 Oklahoma suffered an estimated $1 billion in losses for crop production and $707 million in loss for livestock production due to drought. The 2012 drought losses in Oklahoma reached $239

million for crops, $157 million for livestock, and $27 million in losses due to wildfires (Shideler et al., 2013). Drought related wildfires in state of Oklahoma in the growing burned 59,449 ha in 2011 and 93,012 ha in 2012. The drought of 2011/2012 also led to reduced herd sizes for beef cow operations in the SGP. Beef cow numbers in Texas were reduced by 13.1 % and by 14.3 % in Oklahoma (LMIC, 2012).

Given the potentially severe impacts of drought on grasslands and grazing systems in the SGP, effective decision support tools are needed to assist managers. In order to strengthen the scientific basis for such tools, this dissertation consists of three main projects from which we gained new understanding on the impacts of drought in grasslands and to better predict vegetation dynamics using soil moisture and other vegetation parameters.

I. Accurate estimates of dynamic grassland vegetation parameters, such as above-ground biomass (AGB) and herbaceous fuel moisture content (FMC), are needed in the context of grazing management and wildfire preparedness. AGB and FMC are often measured by hand clipping, which is costly and labor intensive. Ocular estimates of biomass have been used to avoid destructive sampling of AGB in rangelands (Twidwell et al., 2009), but these ocular estimates are subjective and have limited precision. In contrast, spectral reflectance data could potentially provide non-destructive, objective, and relatively inexpensive estimates of AGB and FMC. An attractive feature of reflectance-based methods is their potential,

when combined with satellite observations, to monitor changes on a global scale. For example, Normalized Difference Vegetation Index (NDVI) has been widely used in assessments of grassland biomass. However, when used alone, NDVI showed a weak relationship with standing forage biomass ($r^2 = 0.13$) in tallgrass prairie in Kansas (Olson and Cochran, 1998). In that study, prediction of biomass was improved by also using day of year (DOY) and canopy height (CH). Stepwise multiple linear regression (SMLR) and Artificial Neural Networks (ANN) (Olson and Cochran, 1998) were effective methods for above-ground biomass in a prior study in tallgrass prairie in Kansas, so the aim of the first study in this dissertation was to evaluate the potential for similar nondestructive methods to estimate AGB and FMC in our study area.

II. Fire is an integral part of many SGP ecosystems. Fire helps in nutrient and water cycling, ecosystem restoration, and livestock and timber production (Bidwell et al. 2003). However, wildfires also increase greenhouse gas emissions and cause major economic losses to society (Yebra et al., 2013). According to National Interagency Fire Center (2013), a cost of $2 billion annually has been associated with wildfire loss in the US. Minimizing catastrophic wildfires requires development of improved fire danger assessments. Two critical and poorly understood factors influencing growing season wildfire danger are live fuel moisture content (LFMC) and transition of live fuel to dead fuel. Current fire danger models do not adequately describe LFMC dynamics or live to dead

transitions, but recent evidence suggests both may be strongly influenced by soil moisture conditions. FMC is an important variable in fire ignition and propagation modeling (Pellizzaro et al., 2007), however, direct measurement by oven drying of fresh samples is slow and time consuming. Most of the current fire behavior models predict FMC using weather parameters, or remote sensing indices such as Normalized Difference Vegetation Index (NDVI) and Normalized Difference Water Index (NDWI). The disadvantages associated with satellite images are the low frequency of observations (sometimes weeks to months between readings) and challenges with calibration (Chuvieco et al., 2004c). Some studies suggested that soil moisture measurements have good potential as proxies for FMC (Chuvieco et al., 2009; Krueger et al., 2015; Pellizzaro et al., 2007; Qi et al., 2012). However, there are currently no models capable of dynamic FMC prediction in grasslands using soil moisture information. Therefore, the aims of the second study were to quantify the temporal dynamics of LFMC, live fuel mass, dead fuel mass, and soil moisture expressed as fraction of available water capacity (FAW), and to describe how LFMC and live to dead fuel transition are related to FAW.

III. Rangelands are an important part of grassland ecosystem, characterized by high inter-annual variability in precipitation amounts leading to inter-annual variation in forage production that ultimately determines appropriate stocking rates in grazing livestock production. Accurate and timely forecasts of forage production

several months in advance could be helpful for grazing management, allowing farmers, ranchers, and livestock managers to maintain the sustainability of their operations against adverse conditions such as droughts. Rainfall, soil moisture, and standing crop (measured biomass) have shown potential as predictors of future levels of above-ground biomass in prior studies. Yet, prior studies have not resulted in a proven method for in season forage forecasts informed by soil moisture observations. Such forecasts could be generated using process-based crop simulation models driven by historical or forecasted weather scenarios, if the models effectively described vegetation growth in grazing lands. Therefore, the aim of the third study is to evaluate the performance of the CROPGRO perennial forage model to accurately simulate live mass and soil moisture in grazed tallgrass prairie.

Thesis Outline

The overall objective of this thesis is to improve the ability of researchers and resource managers in the SGP to monitor drought impacts in grasslands and to predict grassland vegetation dynamics using soil moisture information along with other existing information sources. In order to accomplish this overall objective, three distinct projects will be pursued, and a chapter of this thesis will be devoted to each. Those chapters are titled:

1. Nondestructive estimation of aboveground biomass and herbaceous fuel moisture content in tallgrass prairie.
2. Live fuel moisture content and live to dead fuel transitions in Tallgrass Prairie exhibit threshold-type relationships with soil moisture.
3. Preliminary evaluation of a DSSAT model for forage forecasting in Southern Great Plains grasslands.

REFERENCES

Basara, J.B., Maybourn, J.N., Peirano, C.M., Tate, J.E., Brown, P.J., Hoey, J.D., Smith, B.R., 2013. Drought and associated impacts in the Great Plains of the United States—A review. International Journal of Geosciences 4, 72.

Belsky, A.J., Matzke, A., Uselman, S., 1999. Survey of livestock influences on stream and riparian ecosystems in the western United States. Journal of Soil and water Conservation 54, 419-431.

Chuvieco, E., Aguado, I., Dimitrakopoulos, A.P., 2004. Conversion of fuel moisture content values to ignition potential for integrated fire danger assessment. Canadian Journal of Forest Research 34, 2284-2293.

Chuvieco, E., González, I., Verdú, F., Aguado, I., Yebra, M., 2009. Prediction of fire occurrence from live fuel moisture content measurements in a Mediterranean ecosystem. International Journal of Wildland Fire 18, 430-441.

Follett, R.F., Reed, D.A., 2010. Soil carbon sequestration in grazing lands: societal benefits and policy implications. Rangeland Ecology & Management 63, 4-15.

Krueger, E.S., Ochsner, T.E., Engle, D.M., Carlson, J., Twidwell, D., Fuhlendorf, S.D., 2015. Soil moisture affects growing-season wildfire size in the southern great plains. Soil Science Society of America Journal 79, 1567-1576.

LMIC, 2012. Livestock Market Information Center

NASS-USDA, 2012. Census of agriculture. US Department of Agriculture, National Agricultural Statistics Service, Washington, DC.

Olson, K., Cochran, R.C., 1998. Radiometry for predicting tallgrass prairie biomass using regression and neural models. Journal of Range Management, 186-192.

Paruelo, J.M., Lauenroth, W.K., Roset, P.A., 2000. Estimating aboveground plant biomass using a photographic technique. Journal of Range Management, 190-193.

Patrignani, A., Ochsner, T.E., 2015. Canopeo: A Powerful New Tool for Measuring Fractional Green Canopy Cover. Agronomy Journal.

Pellizzaro, G., Cesaraccio, C., Duce, P., Ventura, A., Zara, P., 2007. Relationships between seasonal patterns of live fuel moisture and meteorological drought indices for Mediterranean shrubland species. International Journal of Wildland Fire 16, 232-241.

Qi, Y., Dennison, P., Spencer, J., Riaño, D., 2012. Monitoring live fuel moisture using soil moisture and remote sensing proxies. Fire Ecology 8, 71-87.

Twidwell, D., Fuhlendorf, S.D., Engle, D.M., Taylor Jr, C.A., 2009. Surface fuel sampling strategies: linking fuel measurements and fire effects. Rangeland Ecology & Management 62, 223-229.

Worrall, F., Armstrong, A., Adamson, J., 2007. The effects of burning and sheep-grazing on water table depth and soil water quality in a upland peat. Journal of Hydrology 339, 1-14.

Yebra, M., Chuvieco, E., Riaño, D., 2008. Estimation of live fuel moisture content from MODIS images for fire risk assessment. Agricultural and Forest Meteorology 148, 523-536.

CHAPTER II

NONDESTRUCTIVE ESTIMATION OF ABOVE-GROUND BIOMASS AND HERBACEOUS FUEL MOISTURE CONTENT IN TALLGRASS PRAIRIE

Abstract:

Accurate estimation of above-ground biomass (AGB) and herbaceous fuel moisture content (FMC) are important for grazing management and for wildfire preparedness. Destructive sampling techniques can been used to accurately estimate AGB and FMC, but the process is laborious and time consuming. Therefore, our objective was to develop robust models for nondestructive estimation of AGB and FMC in tallgrass prairie. We calibrated and validated both stepwise multiple linear regression (SMLR) and artificial neural network (ANN) models for AGB and FMC using data collected in grasslands near Stillwater, OK, USA. Day of year, canopy height, Normalized Difference Vegetation Index (NDVI), and percent reflectance at five spectral bands were candidate input variables for the models. Our study spanned two growing seasons and nine patches located within three pastures under patch burn management. For AGB, the ANN and SMLR models performed similarly (RMSE = 110 g m^{-2} versus 114 g m^{-2}). For FMC, the ANN models proved better than SMLR models (RMSE = 23.3% versus RMSE = 27.7%). Given the large variability in the underlying datasets, these models may prove useful for nondestructive estimation of AGB and FMC in other similar grassland environments.

Introduction

Grasslands and grazing systems are essential to agricultural communities in the US Southern Great Plains (SGP) and in similar climatic regions worldwide. More than 55 million ha are classified as grassland or pasture in the SGP states of Kansas, Oklahoma and Texas (NASS, 2012). Accurate estimates of dynamic grassland vegetation parameters are needed for research, grazing management decisions, and wildfire preparedness. Two key parameters in the context of grazing management and wildfire preparedness are above-ground biomass (AGB) and herbaceous fuel moisture content (FMC). Destructive measurement techniques, such as hand clipping have often been used to estimate AGB and FMC at the quadrat scale. Hand clipping is considered to be objective and accurate, but it is also laborious and time consuming, particularly when sampling large, heterogeneous areas. Ocular estimates of biomass have been used to avoid destructive sampling of AGB in rangelands (Twidwell et al., 2009), but these ocular estimates are subjective and have limited precision.

In contrast, spectral reflectance data can potentially provide non-destructive, objective, and relatively inexpensive estimates of AGB and FMC. An attractive feature of reflectance-based methods is their potential, when combined with satellite observations, to monitor changes on a global scale. For example, Normalized Difference Vegetation Index (NDVI) has been widely used in assessments of grassland biomass (Paruelo et al., 1997; Tarr et al., 2005; Zhang et al., 2016). However, when used alone, NDVI showed a

weak relationship with standing forage biomass ($r^2 = 0.13$) in tallgrass prairie in Kansas (Olson and Cochran, 1998). In that study, prediction of biomass was improved by also using day of year (DOY) and canopy height (CH). Similarly, in another study conducted in rangeland in northern California, the plant height-ground cover interaction was strongly correlated with forage biomass with correlation coefficients ranging from 0.538 to 0.988 (Evans and Jones, 1958).

Just as with AGB, the use of nondestructive reflectance-based methods may also overcome some of the obstacles related with field sampling of FMC. For example, FMC on grasslands and shrub lands were accurately estimated (r^2= 0.907 and 0.732) using a 5-year time series (2001-2005) of Terra Moderate Resolution Imaging Spectroradiometer (MODIS) NDVI in Cabañeros National Park in Central Spain (Yebra et al., 2008). Similarly, multitemporal composites derived from four years of NDVI data from the National Oceanic and Atmospheric Administration (NOAA) Advanced Very High Resolution Radiometer (AVHRR) along with surface temperature and day of year were used to estimate FMC (R^2 over 0.8) in Mediterranean grassland in central Spain (Chuvieco et al., 2004b).

Two key methods used to estimate vegetation parameters from reflectance data are stepwise multiple linear regression (SMLR) and Artificial Neural Networks (ANN) (Olson and Cochran, 1998). SMLR is an automated process of building a model by sequentially adding or removing variables based on a specified statistical criterion. An

ANN is a model consisting of multiple interconnected processing elements, called nodes or neurons, that respond dynamically to external inputs (Warner and Misra, 1996). One main advantage of ANNs over SMLR models is that ANNs do not require linear relationships between the variables (Sudheer et al., 2010).

In this study, our objective was to develop robust models for nondestructive estimation of AGB and FMC in tallgrass prairie. We calibrated and validated both stepwise multiple linear regression (SMLR) and artificial neural network (ANN) models for AGB and FMC using data collected in grasslands near Stillwater, OK, USA. Measurements were conducted from May to December of 2012 and from March to November of 2013, and during this time, the sites experienced diverse weather conditions, from drought in the 2012 growing season to normal precipitation during the 2013 growing season.

Materials and Methods

Study area

Research was conducted in tallgrass prairie at the Oklahoma State University Range Research Station located near of Stillwater, Oklahoma. Major vegetation species were little bluestem (*Schizachyrium scoparium* (Michx), big bluestem (*Andropogon gerardii*), Indiangrass (*Sorghastrum nutans*), post oak *(Quercus stellate* (Wang), and eastern redcedar (*Juniperus virginiana*). The dominant soils at this site included the Grainola series (fine, mixed, thermic Vertic Haplustalf) covering approximately 60% of

the area, and the Coyle series (fine-loamy, siliceous, thermic Udic Argiustoll) covering approximately 35% of the area (Gillen et al., 1990).

The study site consisted of three pastures ranging in size from 50 to 63 ha. Those pastures were subdivided into six approximately equal sized unfenced patches. These patches were used in a patch burning treatment designed to increase ecological heterogeneity while preventing woody plant encroachment (Fuhlendorf and Engle, 2004). Each year, two of the six patches were burned: one during the latter months of the dormant season (March-April) and one during the latter months of the growing season (July-October). Patches were burned every three years to represent different successional stages culminating in full recovery for this site after the third year (Fuhlendorf and Engle, 2004). The patch burning sequence has been continuous since the pastures were established in 1999. In the present study, sampling occurred in the patches burned at the end of the growing season. The experimental design was thus a randomized complete block with three treatments, i.e. patches with three different levels of time since burning, and three replications, i.e. the three pastures (Fuhlendorf and Engle, 2004).

In-situ measurements

AGB and FMC were measured at 12 locations in each patch once every two weeks during the 2012 and 2013 growing seasons. Measurements involved hand-clipping all above ground vegetation (both live and dead) in a 0.25-m^2 quadrat, weighing the fresh sample, and drying the vegetation for three days at 70ºC. AGB was calculated on an oven

dry weight basis, and FMC was calculated as the ratio of the weight of water in the sample to its dry weight. Canopy height was also measured at the time of sampling. Canopy reflectance data were collected at each sampling location prior to clipping using a handheld multispectral radiometer (MSR5R, Cropscan, Inc., Rochester, Minnesota, USA) at 2 m above ground between 1200 and 1700 hours. The radiometer measured percentage reflectance in five bands in the 460-1750 nm region (approximate center wavelengths = 485, 560, 660, 830, and 1650 nm). Radiometer calibration was conducted before the start of each growing season using diffusing opal glass, alternately held over the up and down sensors facing the same incident irradiation to calibrate the up and down sensors relative to each other. Normalized Difference Vegetation Index (NDVI) was calculated based on reflectance at wavelengths of 660 and 830 nm (Rouse et al., 1974).

Modeling Procedures

As a preliminary analysis, we performed a simple linear regression of NDVI versus AGB. The purpose of this analysis was to facilitate comparison of our data with the earlier data of Olson and Cochran (1998) and to illustrate the inadequacy of NDVI alone as a predictor of AGB. Subsequently, day of year (DOY), canopy height (CH), percent reflectance in five bands, and Normalized Difference Vegetation Index (NDVI) were used to estimate AGB and FMC using the SMLR model. SMLR fits an observed dependent data set using two or more explanatory variables in a linear equation. SMLR attempts to identify the major variables that influence the dependent variable using a stepwise process of adding and removing terms from a multilinear model. We used the

stepwiselm function in Matlab (2016a, The Mathworks, Inc., Natick, MA). Importance for the candidate independent variables was determined by the *p*-value for the *F*-statistic on the change in the model's sum of squared errors by adding or removing the variables. SMLR starts with only a constant term in the model and then uses forward and backward stepwise regression to construct the final model. The routine adds a variable to the model in a given step if the *p*-value for that variable is less than 0.05 and is the lowest of all the *p*-values for the variables not currently in the model. The fitting process is repeated until no excluded variables have $p < 0.05$. Then the routines remove a variable from the model in a given step if its *p*-value is greater than 0.10 and is the largest of all the *p*-values for the variables in the model. The fitting process is continued until no included variables have $p > 0.10$.

The general equation is as follows:

$$Y = P_0 + P_1 X_1 + ... + P_N X_N \quad [1]$$

where P_i ($i = 0,1, \ldots, N$) are the parameters and X_i ($i = 1,...., n$) are the explanatory variables. We used 85% of the data (randomly selected) for calibration and the remaining 15% for validation. We used the coefficient of determination (R^2), root mean square error (RMSE), adjusted R^2, and bias to evaluate the predictive quality of the models. Lilliefors test was also used to test the model residuals for normality. We used the *lillietest* function in Matlab.

In addition to SMLR, we evaluated the ability of ANNs to estimate AGB and FMC. An ANN is a mathematical structure for representing potentially nonlinear processes by formulating the relationship between inputs and outputs. A three-layer feed-forward network was used with the input layer consisting of eight independent variables (DOY, CH, percent reflectance in five bands, and NDVI). The ANN also included one hidden layer consisting of fifteen neurons, and one output layer. A feed-forward network is an architecture where each variable in the input layer is connected to each neuron in the hidden layer for processing. The processing was accomplished by passing the input signal for each neuron through a hyperbolic tangent transfer function. Each neuron in the hidden layer is also connected to the single neuron in the output layer, which represents the dependent variable, in this case AGB or FMC. A linear transfer function was applied in the output layer. Each connection has a certain weight, a numerical estimation of the connection strength, which is optimized during training. We used the *nntraintool* function in Matlab with the Bayesian regularization-training algorithm to train the model (The Mathworks, Inc., Natick, MA). For the ANN, 70% of the data were used for training (calibration) while 15% of the data were used for the testing phase, which is part of the training process. In the training phase, the network parameters are iteratively adjusted, while the testing phase tests the trained network after each iteration to avoid overfitting to the training data. Training ends when there are no further improvements in predicting the test data. The remaining 15% of the data were used to validate the ANN models. We used

the coefficient of determination (R^2), root mean square error (RMSE), and bias to evaluate the predictive quality of the ANN models. The relative importance of the candidate independent variables was determined based on the connection weights in the trained ANN model using the 'Weight method' as described in Gevrey et al. (2003). For both SMLR and ANN models, we also calculated the RMSE-observations standard deviation ratio (RSR) to allow us to categorize the quality of model performance using the scheme of Moriasi et al. (2007). In addition, we also calculated adjusted R^2 value. The adjusted R^2 value was chosen as it allowed a more fair comparison of SMLR and ANN models with different numbers of independent variables in the models.

Results and Discussion

AGB exhibited large variability in space and time with values ranging from 0 to 852 g m^{-2}. The AGB was positively related to NDVI; however the relationship was relatively weak with an $r^2 = 0.32$ ($p < 0.05$) and RMSE of 191 gm^{-2} (Fig 1). Similarly, AGB was positively but weakly related to NDVI in tallgrass prairie in Kansas (Olson and Cochran, 1998). These results show that NDVI alone cannot be used to accurately estimate AGB in tallgrass prairie. We also tested the multiple regression model described by Olson and Cochran (1998) using NDVI, CH, and DOY for estimating AGB in our dataset. This model proved not to be applicable in our study area ($R^2 = -3.76$ and RMSE of 401 gm^{-2}). $R^2 < 0$ indicates that the mean of the dataset is a better predictor than the

model. This demonstrates the need to develop new and robust models for estimating AGB and FMC.

Stepwise Multiple Linear Regression (SMLR) models

a) Estimation of above-ground biomass (AGB)

DOY, CH, NDVI, and percent reflectance at 560 nm, 660 nm, and 1650 nm were included as significant predictors in the final model for AGB (Table 1). The percent reflectance at 485 nm and 830 nm were insignificant predictors of AGB and not included in the final model directly, although the 830 nm band is used to calculate NDVI. The final model also included several interaction terms between the predictors. In fact, the *p*-value for NDVI was above the exit criterion, but NDVI was retained in the model because of its significant interactions with DOY and 1650 nm reflectance (Table 1). This is consistent with the result shown in Fig. 1 and with the results of Olson and Cochran (1998) who found that NDVI was not strongly related to AGB, but NDVI was retained in their SMLR model to estimate AGB. Although NDVI has been used in prior studies to estimate AGB (r^2 = 0.96 and 0.89 respectively) in grasslands (Anderson et al., 1993; Paruelo et al., 1997), the heterogeneity of the grassland in our study apparently limited the value of NDVI measured at canopy level as a predictor. The patch burn treatment created heterogeneity in both vegetation and grazing pressure. In a similar study with both grazed and ungrazed sites (Todd et al., 1998), NDVI also failed to be significantly related to AGB.

The SMLR model estimated AGB for the validation data with $R^2 = 0.59$ and RMSE = 114 g m^{-2} (Fig. 2). The adjusted R^2 value computed for the validation datasets in the SMLR was 0.59. The SMLR model of Olson & Cochran (1998) which used NDVI, CH, and DOY as predictors achieved a greater $R^2 = 0.83$ and lower RMSE = 73 g m^{-2} on the data set for which it was calibrated. However, that data set spanned only one growing season, included far fewer observations than our data set, and did not include validation data. The SMLR model performance in estimating AGB was classified as satisfactory based on the RSR value of 0.63.

The model underestimated biomass for levels above about 600 g m^{-2}. A Lilliefors test on the residuals indicated that the residuals were not normally distributed ($p < 0.05$). This may be due to the inability of SMLR to describe nonlinear relationships between the predictors and AGB. Estimation of AGB for grasslands with values > 500 g m^{-2} may necessitate the use of nonlinear functions (Pearson et al., 1976). The problem may arise from the radiometer's inability to equally detect reflectance from the lower layers of the canopy. We explored the use of quadratic terms in the SMLR models but they also failed to produce normally distributed residuals. Nonlinear relationships between NDVI and green biomass index have been developed, but these have not yet been adapted for use in multivariate models like the ones in this study (Santin-Janin et al., 2009).

b) Estimation of herbaceous moisture content (FMC)

DOY, CH, NDVI, and percent reflectance at 660 nm, 830 nm, and 1650 nm were included as significant predictors in the final SMLR model for FMC (Table 1). The percent reflectance at 485 nm and 560 nm were excluded in the final model. The final model also included several interaction terms between the predictors. In fact, the *p*-value for CH was above the exit criterion, but CH was included in the model because of significant interactions with DOY, NDVI, and 1650 nm reflectance. For Mediterranean grasslands in Cababeros National Park located in Central Spain, significant predictors for FMC model included integrals of spectral reflectance at 485 nm, 560 nm, 660 nm, 1650 nm, 2200 nm, and the NDVI (Chuvieco et al., 2002b). Spectral reflectance at 2200 nm was not available in our study, but the inclusion of reflectance at 660 nm, 1650 nm, and NDVI in the models from our study and that of Chuvieco et al. (2002b) suggest these three may be useful for FMC estimation in a variety of environments. In the same study , FMC was also estimated effectively using multitemporal analysis of NDVI, surface temperature, and a function of the day of year (Chuvieco et al., 2004b). Thus, inclusion of DOY also appears to be beneficial for FMC estimation across different locations.

The SMLR model estimated FMC for the validation with $R^2 = 0.631$ and RMSE = 27.7% (Fig. 3). The adjusted R^2 value was computed for the validation datasets in SMLR model with a value of 0.63. The SMLR model used in Chuvieco et al. (2002a) estimated FMC with $R^2 = 0.84$ and RMSE = 23.4-40%. Although the R^2 was greater in that study,

our RMSE was within the range that they reported. Their greater R^2 value may be associated with their lower frequency data collection. They used only three reflectance measurements per year from 1996- 1999 with only one measurement in 1999, while in our study, measurements were collected in biweekly intervals. In their follow-up study, FMC was estimated with R^2 over 0.8 and standard error = 31% in grassland (Chuvieco et al., 2004b), which again is comparable to the RMSE from our SMLR model. The SMLR model performance in estimating FMC was classified as satisfactory based on the RSR value of 0.60.

The model underestimated FMC for levels above about 150%. A Lilliefors test on the residuals indicated that the residuals were not normally distributed ($p < 0.05$). This may be due to the inability of SMLR to describe nonlinear relationships between predictors and FMC as we have noted for AGB. Prior research relating spectral reflectance to FMC has also shown that correlation with FMC was strongest at low FMC values < 100% and weaker at high FMC values (Danson and Bowyer, 2004). The authors in that study hypothesized that changes in specific leaf weight and leaf internal structure may be influencing the relationship between FMC and spectral reflectance (Danson and Bowyer, 2004).

Artificial Neural Network (ANN) model

a) Estimation of above-ground biomass (AGB)

As ANN model was better in estimating AGB than an SMLR model in tallgrass prairie in Kansas (Olson and Cochran, 1998), we also wanted to evaluated ANN performance in our datasets. All of the candidate variables (DOY, CH, NDVI, and percent reflectance at 485 nm , 560 nm , 660 nm, 830 nm, and 1650 nm) were included as predictors in the ANN model for estimating AGB because the ANN modeling process did not include a way to eliminate non-significant predictors. Based on the weight method, DOY was the most important independent variable while percent reflectance at 460 nm was the least important variable in the ANN model for AGB (Table 2). These results were consistent with the independent variables retained in the SMLR model where DOY was retained and 460 nm was not retained for estimating AGB (Table 1). For detailed information on the ANN connection weights, see the Appendix.

The fully trained ANN model estimated AGB for the validation data with $R^2 = 0.63$ and RMSE = 109 gm^{-2} (Fig 4.). The adjusted R^2 value computed for the validation datasets in ANN model was 0.63. This ANN model resulted in similar performance as the SMLR model in estimating AGB ($R^2 = 0.63$ vs 0.59, RMSE = 109 g m^{-2} vs 114 g m^{-2}). The ANN model for AGB actually performed substantially better than the SMLR model for the calibration dataset ($R^2 = 0.72$ vs 0.62 and RMSE = 97.8 g m^{-2} vs 114 g m^{-2}), but that performance advantage did not carry over to the validation dataset. The decrease in

performance from the calibration set to the validation set was more pronounced for the ANN model (Fig. 4) than for the SMLR model (Fig. 2). This may indicate some degree of over-fitting the ANN model to the calibration set because of 15 hidden neurons to trained with eight independent variables in the model. Although an ANN model for AGB in tallgrass prairie out-performed an SMLR model in a prior study, neither of those models was tested with an independent validation set (R^2 = 0.79 vs 0.59, RMSE = 70 g m^{-2} vs 103 g m^{-2}) (Olson and Cochran, 1998).

Like the SMLR model, the ANN model also underestimated biomass for levels above 600 g m^{-2}. A Lilliefors test on the residuals indicated that the residuals were not normally distributed ($p < 0.05$). Although the ANN model should be able to account for nonlinearity in the relationships between the predictors and response variable, yet the ANN model did not substantially out-perform the SMLR model for estimating AGB in our study. This could be due to an inadequate number of AGB observations with high biomass levels in the calibration data set for the ANN model. The ANN model performance in estimating AGB was classified as satisfactory based on the RSR value of 0.61. This suggests that there is still further room for improvement in the input data, the ANN structure, or the ANN training process.

b) Estimation of herbaceous moisture content (FMC)

Using the same set of input variables, the fully trained ANN model estimated FMC for the validation set with R^2 = 0.75 and RMSE = 22.7% (Fig. 5). The adjusted R^2

value computed for the valdiation datasets in ANN model was 0.75. DOY was the most important input variable while NDVI was the least important variable in this ANN model for FMC (Table 2). CH was less important for estimating FMC than it was for estimating AGB in both the ANN and SMLR models. An interesting feature was that percent reflectance at 460 nm was the second most important variable in the ANN model for FMC (Table 2), but for the SMLR model, percent reflectance at 460 nm was not retained (Table 1). For detailed information on the ANN model connection weights, see the Appendix. The ANN model showed substantial improvement over the SMLR model in estimating FMC for validation set (R^2 = 0.75 vs 0.63, RMSE = 22.7% vs 27.7%) (Fig. 5 vs Fig. 3). The RMSE for the ANN model estimates of FMC were equal to that of the best SMLR model among those developed by Chuvieco et al. (2004; 2002b). Few, if any, prior studies have directly compared ANN and SMLR models for estimating FMC, and the superior performance of the ANN model in our study suggests ANN models may have good potential for improving FMC estimation in other contexts, e.g. remote sensing of FMC.

Despite the overall good performance of the ANN model for estimating FMC, there was still an underestimation of FMC for values over about 150%. This underestimation again might be due to fewer observations with high values in training the ANN model. A Lilliefors test on the residuals indicated that the residuals were not normally distributed (p<0.05). In addition, we also calculated the RSR to allow us to categorize the quality of

model performance using the scheme of Moriasi et al. (2007). The ANN model performance in estimating FMC was classified as good based on the RSR value of 0.51.

Conclusion

Both the SMLR and ANN models used in our study effectively estimated seasonal changes in above-ground biomass (AGB) and fuel moisture content (FMC). The models, developed from DOY, CH, NDVI, and percent reflectance in five bands, were able to estimate AGB and FMC for tallgrass prairie in Oklahoma with accuracy comparable to that observed in similar studies at other grassland sites. ANN proved better in estimating FMC than SMLR, while for AGB, ANN did not result in substantialy improved estimates in the validation set for our study area. Both types of models underestimated AGB for levels above 600 g m^{-2} and underestimated FMC for levels above 150%. Despite these limitations, the models developed here have been validated using data spanning nine large patches with different burn histories across three different pastures in two years with distinctly different growing conditions. Given this relatively large variance in the underlying datasets, these models should be useful for nondestructive estimation of AGB and FMC in other similar grassland environments, particularly when monitoring large, heterogenous areas for grazing management or wildfire preparedness.

REFERENCES:

Allen, R.G., Pereira, L.S., Raes, D., Smith, M., 1998. Crop evapotranspiration-Guidelines for computing crop water requirements-FAO Irrigation and drainage paper 56. FAO, Rome 300, D05109.

Anderson, G., Hanson, J., Haas, R., 1993. Evaluating landsat thematic mapper derived vegetation indices for estimating above-ground biomass on semiarid rangelands. Remote Sensing of Environment 45.

Basara, J.B., Maybourn, J.N., Peirano, C.M., Tate, J.E., Brown, P.J., Hoey, J.D., Smith, B.R., 2013. Drought and associated impacts in the Great Plains of the United States—A review. International Journal of Geosciences 4, 72.

Belsky, A.J., Matzke, A., Uselman, S., 1999. Survey of livestock influences on stream and riparian ecosystems in the western United States. Journal of Soil and water Conservation 54, 419-431.

Bradshaw, L.S., Deeming, J.E., Burgan, R.E., Jack, D., 1984. The 1978 national fire-danger rating system: technical documentation.

Carlson, J., Burgan, R., 2003. Review of users' needs in operational fire danger estimation: the Oklahoma example. International Journal of Remote Sensing 24, 1601-1620.

Cheney, N., Gould, J., Catchpole, W.R., 1998. Prediction of fire spread in grasslands. International Journal of Wildland Fire 8, 1-13.

Cheney, P., Sullivan, A., 2008. Grassfires: fuel, weather and fire behaviour. CSIRO Publishing.

Chuvieco, E., Aguado, I., Dimitrakopoulos, A.P., 2004a. Conversion of fuel moisture content values to ignition potential for integrated fire danger assessment. Canadian Journal of Forest Research 34, 2284-2293.

Chuvieco, E., Cocero, D., Martín, P., Martínez, J., De la Riva, J., Pérez, F., 2003. Combining NDVI and surface temperature for the estimation of fuel moisture content in forest fire danger assessment, Fourth International Workshop on Remote Sensing and GIS Applications to Forest Fire Management.

Chuvieco, E., Cocero, D., Riano, D., Martin, P., Martınez-Vega, J., de la Riva, J., Pérez, F., 2004b. Combining NDVI and surface temperature for the estimation of live fuel moisture content in forest fire danger rating. Remote Sensing of Environment 92, 322-331.

Chuvieco, E., Cocero, D., Riaño, D., Martin, P., Martínez-Vega, J., de la Riva, J., Pérez, F., 2004c. Combining NDVI and surface temperature for the estimation of live fuel moisture content in forest fire danger rating. Remote Sensing of Environment 92, 322-331.

Chuvieco, E., González, I., Verdú, F., Aguado, I., Yebra, M., 2009. Prediction of fire occurrence from live fuel moisture content measurements in a Mediterranean ecosystem. International Journal of Wildland Fire 18, 430-441.

Chuvieco, E., Riano, D., Aguado, I., Cocero, D., 2002a. Estimation of fuel moisture content from multitemporal analysis of Landsat Thematic Mapper reflectance data: applications in fire danger assessment. International Journal of Remote Sensing 23, 2145-2162.

Chuvieco, E., Riaño, D., Aguado, I., Cocero, D., 2002b. Estimation of fuel moisture content from multitemporal analysis of Landsat Thematic Mapper reflectance data: Applications in fire danger assessment. International Journal of Remote Sensing 23, 2145-2162.

Danson, F., Bowyer, P., 2004. Estimating live fuel moisture content from remotely sensed reflectance. Remote Sensing of Environment 92, 309-321.

Ellsworth, L., Dale, A., Litton, C., Miura, T., 2017. Improved fuel moisture prediction in non-native tropical Megathyrsus maximus grasslands using Moderate-Resolution Imaging Spectroradiometer (MODIS)-derived vegetation indices. International Journal of Wildland Fire 26, 384-392.

Evans, R.A., Jones, M.B., 1958. Plant height times ground cover versus clipped samples for estimating forage production. Agronomy Journal 50, 504-506.

Follett, R.F., Reed, D.A., 2010. Soil carbon sequestration in grazing lands: societal benefits and policy implications. Rangeland Ecology & Management 63, 4-15.

Ford, T.W., McRoberts, D.B., Quiring, S.M., Hall, R.E., 2015. On the utility of in situ soil moisture observations for flash drought early warning in Oklahoma, USA. Geophysical Research Letters 42, 9790-9798.

Fuhlendorf, S., Engle, D., 2004. Application of the fire–grazing interaction to restore a shifting mosaic on tallgrass prairie. Journal of Applied Ecology 41, 604-614.

Gevrey, M., Dimopoulos, I., Lek, S., 2003. Review and comparison of methods to study the contribution of variables in artificial neural network models. Ecological Modelling 160, 249-264.

Gillen, R.L., McCollum, F.T., Brummer, J.E., 1990. Tiller defoliation patterns under short duration grazing in tallgrass prairie. Journal of Range Management, 95-99.

Gillen, R.L., Tate, K.W., 1993. The constituent differential method for determining live and dead herbage. Journal of Range Management, 142-147.

Hoerling, M., Eischeid, J., Kumar, A., Leung, R., Mariotti, A., Mo, K., Schubert, S., Seager, R., 2014. Causes and predictability of the 2012 Great Plains drought. Bulletin of the American Meteorological Society 95, 269-282.

Krueger, E.S., Ochsner, T.E., Carlson, J., Engle, D.M., Twidwell, D., Fuhlendorf, S.D., 2016. Concurrent and antecedent soil moisture relate positively or negatively to probability of large wildfires depending on season. International Journal of Wildland Fire 25, 657-668.

Krueger, E.S., Ochsner, T.E., Engle, D.M., Carlson, J., Twidwell, D., Fuhlendorf, S.D., 2015. Soil moisture affects growing-season wildfire size in the southern great plains. Soil Science Society of America Journal 79, 1567-1576.

LMIC, 2012. Livestock Market Information Center

Moriasi, D.N., Arnold, J.G., Van Liew, M.W., Bingner, R.L., Harmel, R.D., Veith, T.L., 2007. Model evaluation guidelines for systematic quantification of accuracy in watershed simulations. Trans. Asabe 50, 885-900.

NASS-USDA, 2012. Census of agriculture. US Department of Agriculture, National Agricultural Statistics Service, Washington, DC.

Ochsner, T.E., Cosh, M.H., Cuenca, R.H., Dorigo, W.A., Draper, C.S., Hagimoto, Y., Kerr, Y.H., Njoku, E.G., Small, E.E., Zreda, M., 2013. State of the art in large-scale soil moisture monitoring. Soil Science Society of America Journal 77, 1888-1919.

Olson, K., Cochran, R.C., 1998. Radiometry for predicting tallgrass prairie biomass using regression and neural models. Journal of Range Management, 186-192.

Paruelo, J.M., Epstein, H.E., Lauenroth, W.K., Burke, I.C., 1997. ANPP Estimates from NDVI for the Central Grassland Region of the United States. Ecology 78, 953-958.

Pearson, R.L., Miller, L.D., Tucker, C.J., 1976. Hand-held spectral radiometer to estimate gramineous biomass. Appl. Opt. 15, 416-418.

Pellizzaro, G., Cesaraccio, C., Duce, P., Ventura, A., Zara, P., 2007. Relationships between seasonal patterns of live fuel moisture and meteorological drought indices for Mediterranean shrubland species. International Journal of Wildland Fire 16, 232-241.

Qi, Y., Dennison, P., Spencer, J., Riaño, D., 2012. Monitoring live fuel moisture using soil moisture and remote sensing proxies. Fire Ecology 8, 71-87.

Rouse , J., Haas, R., Schell, J., Deering, D., 1974. Monitoring Vegetation Systems in the Great Plains with Erts. NASA Special Publication 351, 309.

Rouse Jr, J., Haas, R., Schell, J., Deering, D., 1974. Monitoring Vegetation Systems in the Great Plains with Erts. NASA Special Publication 351, 309.

Santin-Janin, H., Garel, M., Chapuis, J.-L., Pontier, D., 2009. Assessing the performance of NDVI as a proxy for plant biomass using non-linear models: a case study on the Kerguelen archipelago. Polar Biology 32, 861-871.

Scott, B.L., Ochsner, T.E., Illston, B.G., Fiebrich, C.A., Basara, J.B., Sutherland, A.J., 2013. New Soil Property Database Improves Oklahoma Mesonet Soil Moisture Estimates*. Journal of Atmospheric and Oceanic Technology 30, 2585-2595.

Scott, J.H., Burgan, R.E., 2005. Standard fire behavior fuel models: a comprehensive set for use with Rothermel's surface fire spread model. The Bark Beetles, Fuels, and Fire Bibliography, 66.

Sudheer, K., Gowda, P., Chaubey, I., Howell, T., 2010. Artificial neural network approach for mapping contrasting tillage practices. Remote Sensing 2, 579-590.

Tarr, A.B., Moore, K.J., Dixon, P.M., 2005. Spectral reflectance as a covariate for estimating pasture productivity and composition. Crop science 45, 996-1003.

Todd, S., Hoffer, R., Milchunas, D., 1998. Biomass estimation on grazed and ungrazed rangelands using spectral indices. International Journal of Remote Sensing 19, 427-438.

Twidwell, D., Fuhlendorf, S.D., Engle, D.M., Taylor Jr, C.A., 2009. Surface fuel sampling strategies: linking fuel measurements and fire effects. Rangeland Ecology & Management 62, 223-229.

Wang, M., Yang, B., Hu, F., Zang, X., 2014. On-orbit geometric calibration model and its applications for high-resolution optical satellite imagery. Remote Sensing 6, 4391-4408.

Warner, B., Misra, M., 1996. Understanding neural networks as statistical tools. The american statistician 50, 284-293.

Worrall, F., Armstrong, A., Adamson, J., 2007. The effects of burning and sheep-grazing on water table depth and soil water quality in a upland peat. Journal of Hydrology 339, 1-14.

Yebra, M., Chuvieco, E., Riaño, D., 2008. Estimation of live fuel moisture content from MODIS images for fire risk assessment. Agricultural and Forest Meteorology 148, 523-536.

Yebra, M., Dennison, P.E., Chuvieco, E., Riaño, D., Zylstra, P., Hunt, E.R., Danson, F.M., Qi, Y., Jurdao, S., 2013. A global review of remote sensing of live fuel moisture content for fire danger assessment: Moving towards operational products. Remote Sensing of Environment 136, 455-468.

Zhang, C., Lu, D., Chen, X., Zhang, Y., Maisupova, B., Tao, Y., 2016. The spatiotemporal patterns of vegetation coverage and biomass of the temperate deserts in Central Asia and their relationships with climate controls. Remote Sensing of Environment 175, 271-281.

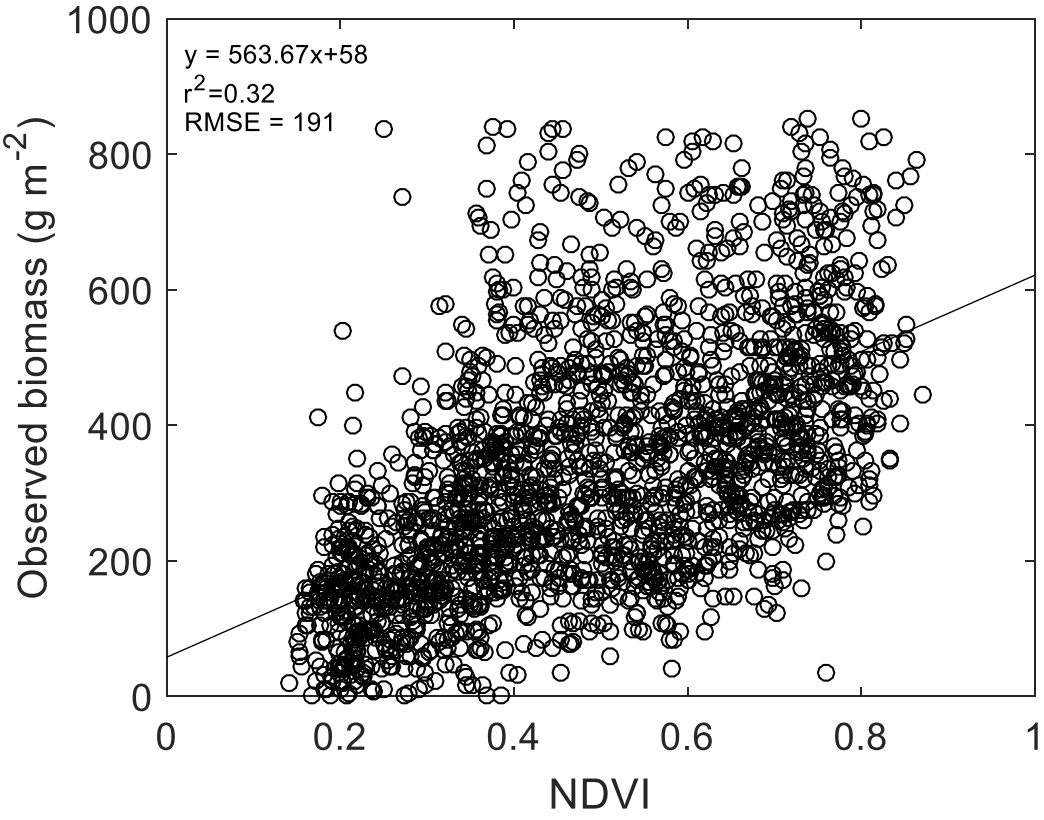

Fig. 1: Linear regression of aboveground biomass (AGB) versus Normalized Difference Vegetation Index (NDVI)

Table 1: Independent variables retained in stepwise multiple regression models for AGB (aboveground biomass) and FMC (herbaceous moisture content) along with corresponding parameter estimate, standard errors (SE), and *p*-values. The independent variables are day of year (DOY), canopy height (CH), normalized difference vegetation index (NDVI), and spectral reflectance at different wavelengths.

	AGB (g m^{-2})			FMC (%)		
Ind. Variables	Estimate	SE	*p*-values	Estimate	SE	*p*-values
Intercept	-249	93	0.007	62.5	29.2	0.03
DOY	-0.58	0.11	< 0.00	0.18	0.07	0.015
CH (m)	472	110	< 0.001	9.46	45.4	0.83
NDVI	69.5	134	0.6	205	32.9	<0.001
560 nm (%)	43.7	8.8	< 0.001			
660 nm (%)	-25.6	3.99	< 0.001	-5.45	2.655	0.04
830 nm (%)				1.52	0.289	< 0.001
1650 nm (%)	17.8	3.24	< 0.001	-3.73	0.475	< 0.001
DOY × CH	-0.67	0.32	0.04	0.44	0.073	< 0.001
DOY × NDVI	3.4	0.36	< 0.001	-0.72	0.095	< 0.001
DOY × 660 nm				-0.009	0.005	0.06
CH × NDVI				-110.3	32.348	< 0.001
CH × 1650 nm				-4.78	0.995	< 0.001
NDVI × 660 nm				11.7	2.006	< 0.001
CH × 660 nm	29.1	8.52	< 0.001			
NDVI × 1650 nm	-21.4	4.04	< 0.001			
560 nm × 1650 nm	-0.7	0.28	0.02			
660 nm × 1650 nm				0.18	0.042	< 0.001

Table 2: Relative importance (RI) of various independent variables in trained Artificial Neural Network for AGB and FMC. The relative importance is shown as percentage. The independent variables are day of year (DOY), canopy height (CH), normalized difference vegetation index (NDVI), and percent reflectance at five spectral bands.

	DOY	CH	NDVI	460 nm	560 nm	660 nm	830 nm	1650 nm
		m		%	%	%	%	%
AGB	15.0	13.7	11.38	9.24	12.0	14.9	10.41	13.1
FMC	17.7	11.6	10.11	14.5	11.1	10.5	11.2	13.27

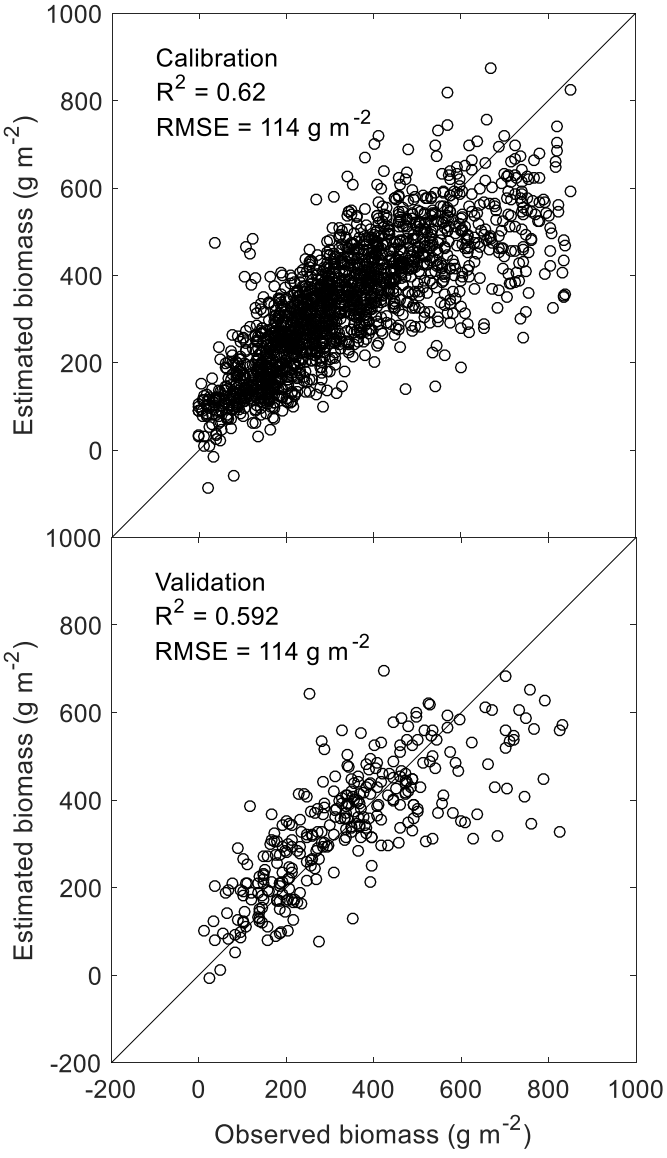

Fig. 2. Estimation of above-ground biomass (AGB) using stepwise multiple linear regression. Candidate independent variables included NDVI, canopy height, day of year and all the five spectral bands. The model was calibrated using 85% of the data and validated using the remaining 15%.

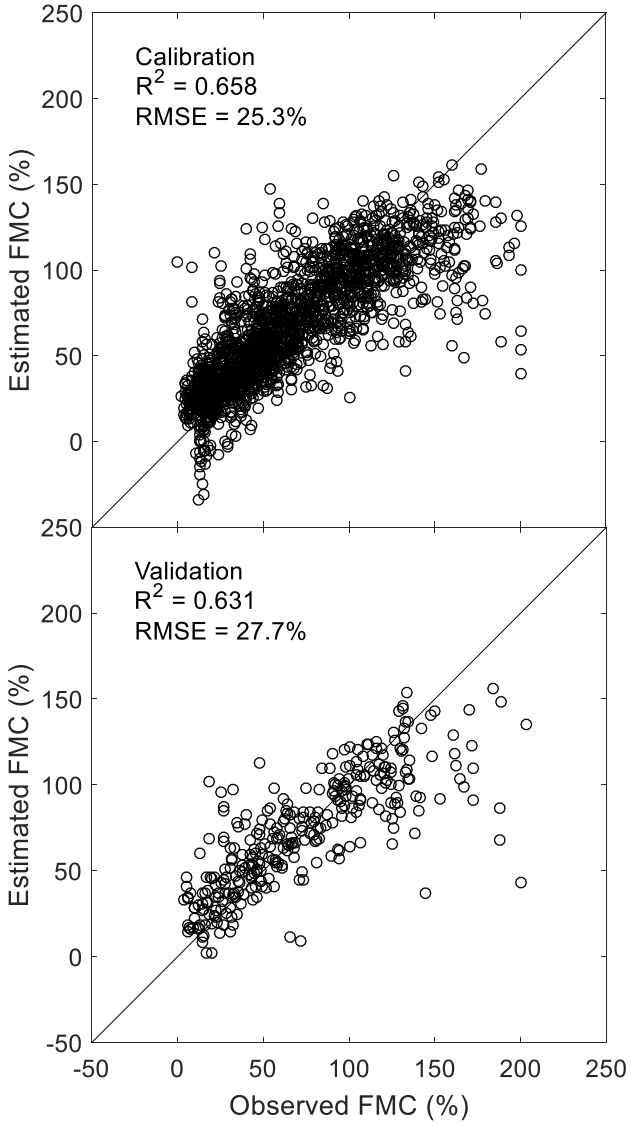

Fig 3. Estimation of fuel moisture content (FMC) using stepwise multiple linear regression. Candidate independent variables included NDVI, canopy height, day of year and all the five spectral bands. The model was calibrated using 85% of the data and validated using the remaining 15%.

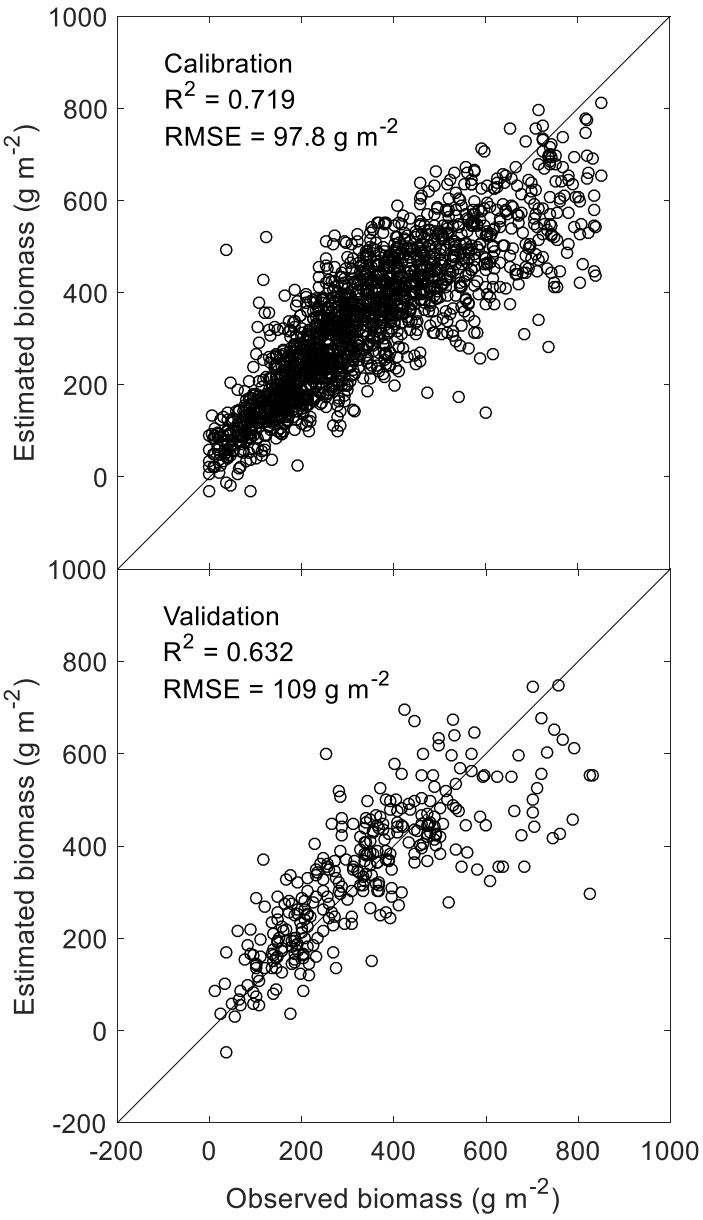

Fig. 4. Estimation of above-ground biomass (AGB) using artificial neural network. Candidate independent variables included NDVI, canopy height, day of year and all the five spectral bands. The model was calibrated using 85% of the data and validated using the remaining 15%.

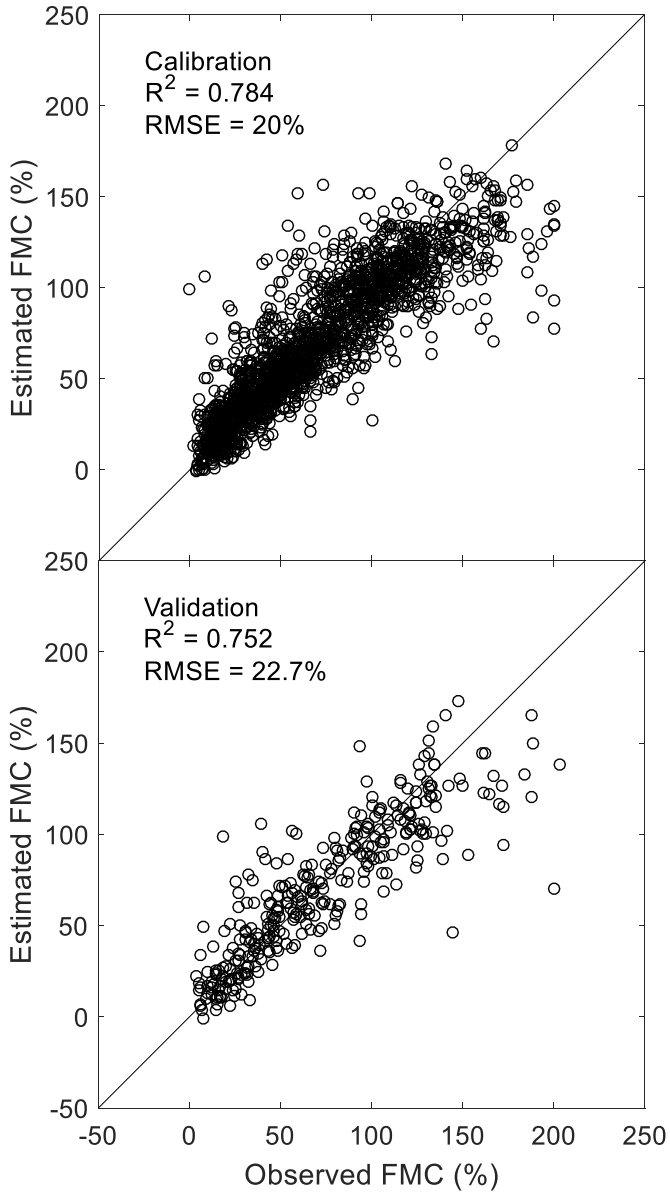

Fig. 5. Estimation of fuel moisture content (FMC) using artificial neural network. Candidate independent variables included NDVI, canopy height, day of year and all the five spectral bands. The model was calibrated using 85% of the data and validated using the remaining 15%.

CHAPTER III

LIVE FUEL MOISTURE CONTENT AND LIVE TO DEAD FUEL TRANSITIONS IN TALLGRASS PRAIRIE EXHIBIT THRESHOLD -TYPE RELATIONSHIP WITH SOIL MOISTURE

Abstract:

Fire is an integral part of grassland ecosystems, exerting a strong influence on ecosystem processes, biodiversity, and livestock production, but, wildfires cause major socio-economic losses in regions such as the US Great Plains. Two critical and poorly understood factors influencing growing season wildfire danger are live fuel moisture content (LFMC) and transition of live fuel to dead fuel. Current fire danger models do not adequately describe LFMC dynamics or live to dead transitions, but recent evidence suggests both may be strongly influenced by soil moisture conditions. Therefore, the objectives of this study were i) to quantify the temporal dynamics of LFMC, live fuel mass, dead fuel mass, and soil moisture expressed as fraction of available water capacity (FAW), and ii) to describe how LFMC and live to dead fuel transition are related to FAW. During the growing seasons of 2012-13, LFMC, live mass, dead mass, and FAW were monitored in tallgrass prairie under patch burn management near Stillwater, OK. LFMC exhibited a nonlinear, threshold-type relationship with FAW, with LFMC being insensitive to FAW at FAW levels above approximately 0.56 and positively related to

FAW below that threshold. Live to dead fuel transitions occurred around a FAW value of approximately 0.34, with the rate of transition increasing linearly as FAW dropped below that threshold. In light of these findings and the increasing availability of soil moisture data, a logical next step would be to develop ways to incorporate soil moisture information into dynamic fuel bed models for improved fire danger assessments and enhanced wildfire preparedness.

Introduction

Fire is an integral part of grassland ecosystems worldwide, exerting a strong influence on ecosystem processes including nutrient and water cycling and ecosystem services including biodiversity and livestock production. However, wildfires also increase greenhouse gas emissions and cause major economic losses to society (Yebra et al., 2008). According to the National Interagency Fire Center (2013), a cost of $2 billion annually has been associated with wildfire loss in the US. The US Southern Great Plains, with its strong winds and frequent droughts, is a region where wildfire is a significant threat. A single group of wildfires (the NW Oklahoma Complex) in March 2017, burned over 337 thousand ha in Oklahoma and Kansas (Wildfire Today, 2017) and resulted in almost $15 million in losses to the Oklahoma cattle industry alone (OSU Extension, 2017). There were eighteen large wildfires in Arizona, Utah, California, New Mexico, Nevada and Oregon burning over 1 million ha during the first seven months of 2017 (NIFC, 2017)Minimizing wildfire damages requires development of improved fire danger

assessments (Yebra et al., 2013). One approach to improving those assessments is through better monitoring of changes in fuel moisture content.

Fuel moisture content (FMC) is an important variable driving fire ignition and fire spread (Cheney and Sullivan, 2008) and FMC is a key input variable in models of ignition and propagation (Pellizzaro et al., 2007). However, direct measurement of FMC by oven drying of fresh samples is slow and time consuming. Currently, estimates of FMC in fire danger assessments are based on static fuel models, weather data, or vegetation indices from satellite remote sensing. Weather data are mainly used to estimate the moisture content of dead fuels important to ignition and the spread of wildfires (Cheney et al., 1998). However, live fuel moisture and the transition of live fuel to dead fuel, also important contributors to ignition and spread potential, are less well understood and difficult to obtain, and therefore are generally included in fire models in simple forms such as heuristic variables. State and national fire danger systems have used weather factors such as air temperature, relative humidity and wind speed to assess wildfire danger rating, but neither system captures the dynamic nature of LFMC and the transition of live fuel to dead fuel (Bradshaw et al., 1984; Carlson and Burgan, 2003).

Satellite data have been used to estimate live fuel moisture content (LFMC). The better spatial coverage provided by satellite images provides advantages over weather data for estimating LFMC across large areas. LFMC values have shown statistically significant correlations with remote sensing indices such as Normalized Difference Vegetation Index (NDVI) and Normalized Difference Water Index (NDWI) in

Mediterranean species of grasslands and shrublands (Chuvieco et al., 2003; Chuvieco et al., 2004c; Yebra et al., 2008). However, satellite images have disadvantages such as low frequency of observations (sometimes weeks to months between readings) and challenges with calibration to ground truth data (Chuvieco et al., 2004a; Wang et al., 2014). There is a clear need for better method to describe dynamics of spatially and temporally variable LFMC.

Soil moisture has potential to serve as a useful predictor for LFMC in fire danger assessments. In North Western Sardinia in Italy, soil moisture was more highly correlated with LFMC than weather variables for four Mediterranean shrubs species (Pellizzaro et al., 2007). Likewise, soil moisture was also more strongly related with LFMC for shrub species of Gambel oak and big sagebrush than was remotely sensed NDVI or NDWI across ten sites in northern Utah, USA (Qi et al., 2012). A strong relationship between soil moisture in form of fraction of available water capacity (FAW) and growing-season wildfire size in Oklahoma provides indirect evidence that soil moisture may strongly influence LFMC and the transition from live fuel to dead fuel during the growing season (Krueger et al., 2015). Soil moisture also played a major role in controlling the probability of large growing-season wildfires in Oklahoma (Krueger et al., 2016). The development of large-scale soil moisture monitoring networks (Ochsner et al., 2013) has provided the opportunity to use soil moisture data to estimate LFMC and the transition from live fuel to dead fuel.

Considering this, we aimed to assess the potential of using FAW to enable early warning of rapidly declining LFMC and the transition from live fuel to dead fuel in the growing season of grasslands dominated by warm-season grasses. The specific objectives of this study were i) to quantify the temporal dynamics of LFMC, live fuel mass, and dead fuel mass, and FAW, and ii) to describe how LFMC, and live to dead fuel transition are related to FAW.

Materials and Methods

Research was conducted at the Oklahoma State University Range Research Station (Lat = 36.06, Lon = -97.21) located near of Stillwater, Oklahoma. The location is primarily tallgrass prairie dominated by warm-season grasses. Major vegetation species were little bluestem (*Schizachyrium scoparium* Michx), big bluestem (*Andropogon gerardii*), Indiangrass (*Sorghastrum nutans*), post oak (*Quercus stellate* Wang), and eastern redcedar (*Juniperus virginiana*). The predominant soils at this site included the Grainola series (fine, mixed, thermic Vertic Haplustalf) covering approximately 60% of the area, and the Coyle series (fine-loamy, siliceous, thermic Udic Argiustoll) covering approximately 35% of the area (Gillen et al., 1990). The study site consists of three pastures ranging in size from 50 to 63 ha. Those pastures were subdivided into six approximately equal sized unfenced patches. These patches were used to apply a patch burning treatment designed to increase ecological heterogeneity while preventing woody plant encroachment (Fuhlendorf and Engle, 2004). Each year, two of the six patches were burned: one during the late dormant season (February-April) and one during the late

growing season (July-October). Patches were burned every three years to represent different successional stages culminating in full recovery for this site after the third year (Fuhlendorf and Engle, 2004). The patch burning sequence has been continuous since the pastures were established in 1999. In the present study, sampling occurred in the three patches in each pasture that were burned during the growing season for a total of nine patches (Fuhlendorf and Engle, 2004). Each pasture was moderately grazed by cattle and cattles were grazing freely either on burned or unburned patches.

Data collection

LFMC, live fuel mass, and dead fuel mass were measured every two weeks in each patch during the growing season for years 2012 and 2013. The growing season was defined as the months of May through October. Twelve vegetation samples in randomly selected 0.25 m^2 quadrats were clipped after noon in each of the nine patches during each sampling period. LFMC for each patch and sampling period was calculated as the mean value of fuel moisture content of six pure live herbaceous sub-samples. The mixture of live and dead herbaceous material were clipped from each quadrat, collected, weighed, and dried in a 70°C drying oven for 48 h. The percentage of live and dead in each sample was calculated based on the constituent differential method (Gillen and Tate, 1993). This method is based on the difference in moisture content of pure live and pure dead subsamples. Live mass was calculated as the product of the proportion of live fuel in the

mix and the dry weight of each quadrat sample, whereas dead mass is calculated as the product of the proportion of dead fuel in the mix and the sample mass.

Soil moisture in form of volumetric water content was measured hourly at four different depths (i.e. 5, 10, 20 and 50 cm) using reflectometry-based sensors (Model 655, Campbell Scientific, Logan, UT) installed at one location in each sample patch in all three pastures. The soil moisture sensors were calibrated using Coyle-Lucien complex soil obtained from one of the patches (36.06142ºN, 97.21727ºW). Soil properties were determined from the soil sampling done on March 13, 2013. The soil properties measured included volumetric water content retained at -10 and at -1500 k Pa. Fraction of available water capacity (FAW) was calculated based on the daily-averaged volumetric water content and the measured soil properties. Trapezoidal numerical integration was used to calculate FAW for the 0–40 cm layer as follows:

$$FAW = \frac{1}{L}\int_{0}^{L}\frac{\theta(Z)-\theta(WP)}{\theta_{FC}(Z)-\theta_{WP}(Z)}dz \qquad [1]$$

where θ is measured volumetric water content, θ_{WP} is volumetric content at permanent wilting point estimated at -1500 k Pa; θ_{FC} is the volumetric water content at field capacity estimated at -10 k Pa, and z represents the soil depth. L represents the maximum depth of interest. Values of FAW are typically between 0 (no plant available soil water) and 1 (maximum available water capacity is filled). Values of FAW less than approximately 0.5 typically indicate conditions of vegetative moisture stress (Allen et al., 1998). In addition,

reference evapotranspiration (ET_0) was obtained using FAO-56 method (Allen et al. 1998) from weather data including maximum and minimum air temperature (˚C), minimum and maximum relative humidity (%), average wind-speed (m s^{-1}), rainfall (mm), and solar radiation (W m^{-2}) at the Marena Mesonet site (McPherson et al., 2007).

Data Analysis

Because the patch burning treatment can dramatically alter the fuel bed properties, the vegetation and soil data were composited for each level of time since fire. In each growing season, there are three patches in their first year since fire, three in their second year, and three in their third year. The time series of LFMC (%), live mass (g m^{-2}), dead mass (g m^{-2}), and FAW were plotted to visualize the relationship between the variables. The relationship of LFMC and FAW was described using a box and whisker plot as described in Krueger et al. (2015). Live fuel moisture content classes were assigned as 0-100%, 100-200%, 200-300%, 300-400%, and 400-500%. The relationship between live fuel mass and cumulative FAW was also evaluated with a box and whisker plot. Live mass classes were assigned as 0-50 g m^{-2}, 50- 150 g m^{-2}, 150-250 g m^{-2}, 250-350 g m^{-2} , and >350 g m^{-2}. For live mass, the data were taken from the patches in their second and third year since fire because the lack of standing dead fuel in the first year after fire alters the live mass accumulations. The changes in live and dead mass between sampling dates for each patch were calculated to find the transition of live to dead fuel. Identifying these transition period allowed us to estimate the critical threshold of FAW where live fuel

transitioned to dead fuel. Transition periods were defined as intervals when live mass decreased and dead mass increased. The FAW during each of these intervals was determined. We also plotted time series ET_O and precipitation for two calendar years for comparing with time series response of LFMC, live and dead mass.

Results

Weather Conditions

Cumulative precipitation was approximately 50 mm above average by end of April 2012, creating favorable conditions for early season vegetative growth. However, below average rainfall in end of May 2012 resulted in cumulative precipitation falling below average by the start of June. That precipitation deficit increased through June and July, and the deficit reached approximately150 mm by end of July before abating slightly following rain in mid-August. By end of 2012, the cumulative precipitation was approximately 300 mm below average (Fig. 1). The low precipitation corresponded with high temperatures as reflected in the relatively high reference ET values for 2012 (Fig. 2). The atmospheric water deficit (ET-P) reached approximately 1600 mm by end of 2012. In contrast, cumulative precipitation was near or above average throughout 2013, reference ET was lower than in 2012 because of lower temperatures, and the end of year atmospheric water deficit was only approximately 400 mm (Fig. 2).

Fraction of Available Water Capacity

Sampling began on 22 May 2012 after the start of the period of below average precipitation, so the initial FAW measurements were < 0.6. FAW reached a maximum value of 0.67 on 5 June 2012 then declined steadily until 14 August 2012 as drought conditions developed. FAW fell below 0.5 on 20 June 2012. Minimum FAW values were below 0.2. After rainfall totaling 67 mm between 25 August and 26 August, FAW briefly increased to > 0.5 on 29 August 2012, but dropped again to < 0.3 by 12 September 2012, and remained low for the rest of the growing season (Fig. 3a). In 2013, FAW reached maximum values above 0.9 on 11 June 2013 and did not drop below 0.5 until 8 July 2013, 18 days later than in 2012. July and August rainfall caused FAW to increase through July and August. However, dry conditions in September caused a secondary decline in FAW, reaching a minimum of 0.17 on 16 September 2013 (Fig. 3b).

Live Fuel Moisture Content

In 2012, the maximum LFMC value of 206% was recorded on the first sampling date 24 May 2012. A relatively large drop in LFMC occurred between the second and third sampling dates as FAW value decreased from > 0.6 to < 0.6. The minimum recorded LFMC values occurred during the first three weeks of August 2012 when LFMC was < 100%, coincident with the minimum values of FAW (Fig 3c). Low (<100%) LFMC occurred relatively in the early growing season in 2012. In 2013, the maximum LFMC of 879% was again recorded on the first sampling date of the growing

season, 13 May 2013. LFMC declined as the season progressed until stabilizing at values of ~200% through July and August. LFMC never fall below 100% in 2013. The minimum was 128% on 19 Oct 2013, as the vegetation senesced at the end of growing season (Fig 3d). The patches burned in October 2012 had much lower LFMC values than the other patches in May-August of 2013.

Live mass

Above average rainfall and relatively warm temperatures produced rapid early growth in 2012, with live mass of 141 gm^{-2} on the first sampling date 24 May 2012. Live mass increased until 20 June 2012, reaching peak values > 200 g m^{-2}, and then declined until mid-August as drought developed and FAW dropped. Minimum live mass for 2012 was 46.7 g m^{-2} on 14 August 2012 (Fig. 3e) In 2013, cooler spring temperatures resulted in lower levels of initial live mass, but live mass increased continuously from May- August, reaching maximum values > 200 g m^{-2} in August and early September. Live mass dropped sharply in mid-September and early October 2013, and FAW fell to < 0.2 during this same time period. The patches burned on 15 October 2012, had higher live biomass than the other patches from May- September 2013 (Fig. 3f).

Dead mass

In 2012, dead mass increased dramatically in July as FAW fell below 0.4, after that dead mass was relatively constant with values of 200-300 g m^{-2} until the end of growing season in 2012. In 2013, after the controlled burn on 15 October 2012, the dead

mass remained in the recently burned patch was zero until 22 August 2013 (Fig. 3g). The dead mass in the recently burned patches increased to > 300 g m^{-2} in September 2013 after FAW dropped below 0.2. The dead mass was higher at the starting of growing season for the patches which were not burned in October 2012, but these patches also showed an increased in dead mass during September 2013 (Fig. 3h).

Relationship of LFMC and FAW

LFMC > 300% coincided with FAW > 0.7, and LFMC < 100% coincided with FAW <0.35. LFMC was sensitive to FAW at low FAW values but was insensitive above some threshold of FAW. The threshold below which LFMC is sensitive to FAW was estimated using the average of the FAW values for the third LFMC category (200-300%), in the sensitive range, and the fourth LFMC categories (300-400%), the insensitive range. The estimated FAW threshold for LFMC sensitivity was 0.56 (Fig. 4).

Relationship of Live to dead fuel transition and FAW

The maximum rate of live to dead fuel transition reached 17 g m^{-2} d^{-1} when FAW during the interval between sampling events averaged 0.19. The average FAW value at which live to dead fuel transitions occurred was 0.34. There is an apparently linear relationship between FAW and transition rate below this threshold. As FAW decreases, the rate of transition from live to dead increases (Fig. 5). Similarly, LFMC values < 100% only occurred when FAW was < 0.34 (Fig. 4).

Discussion

The severe drought in 2012 and near average weather conditions in 2013 provided an ideal environment for studying the relationship between LFMC and FAW and the influence of FAW on live to dead fuel transitions. The precipitation deficits in the Central Great Plains during May-August 2012 were more severe than any in the past century, including the Dust Bowl years (Hoerling et al., 2014). This rapid-onset (flash) drought was reflected in soil moisture data from Oklahoma Mesonet stations across central and eastern Oklahoma (Ford et al., 2015), with statewide average FAW values below 0.2 in July and August 2012 (Krueger et al., 2015).The drought conditions led to major growing season wildfire outbreaks with 93,043 ha burned across the state (Krueger et al., 2015).

The grassland LFMC levels observed in this study are generally consistent with previously reported values, showing the expected phenologically-driven decline from the start to the end of the growing season (Chuvieco et al., 2009). The high moisture content of the tissues produced in early vegetative growth gives way to lower moisture content as the tissues mature. The maximum LFMC values (>400%) in this study are high relative to those in prior studies. For example, in grasslands in Hawaii, LFMC varied between 45 and 294% (Ellsworth et al., 2017). The higher values observed here may be related to the constituent difference sampling method used, which relied on direct measurements of pure live sub-samples. The live mass values observed here are also consistent with those in prior studies in similar environments. For example, a previous study of tallgrass prairie

at the same research station resulted in live standing crop estimates ranging from 84 to 387 g m^{-2} (Gillen and Tate, 1993).

Grassland LFMC values displayed a threshold-type response to measured soil moisture in this study, in contrast to the simple linear relationships which have been previously reported for other fuel types. For example, in Italy, LFMC of four shrub species was positively correlated with soil moisture ($r > 0.6$) (Pellizzaro et al., 2007). Likewise, LFMC for Gambel oak (*Quercus gambelii* Nutt) and big sagebrush (*Artemisia tridentate* Nutt) in Utah showed positive linear relationships with measured soil moisture, stronger relationships than observed for LFMC and various remotely-sensed vegetation indices (Qi et al., 2012). Grassland LFMC became sensitive to soil moisture only after FAW dropped below a threshold of approximately 0.56. The nonlinear response of LFMC to FAW may help to explain the previously reported nonlinear relationship between FAW and wildfire probability in Oklahoma (Krueger et al., 2016). In that study, the probability of large wildfire, on a day with low relative humidity and high wind speed, increased nonlinearly from 0.18 to 0.60 as FAW decreased from 0.5 to 0.2. Indeed most large wildfires in Oklahoma occur when FAW < 0.2 (Krueger et al., 2015), conditions capable of producing LFMC < 100% in this study.

We hypothesize that the lowest category of grassland LFMC values (0-100%) is strongly controlled by FAW, while intermediate LFMC values (100-300%) occur across a wider range of FAW suggesting multiple controlling factors. We hypothesize that these

intermediate levels of FAW are influenced by the interactions of phenology, available soil moisture, and atmospheric water demand, i.e. reference ET. The highest LFMC values (>300%) are likely strongly influenced by phenology as they occur only in the early growing season.

The relationship between LFMC and FAW suggests some new possibilities for modeling the dynamics of fuel behavior. The standard fire behavior fuel models (Scott and Burgan, 2005) describes the concept of live herbaceous load transferred to dead as function of LFMC, but does not indicate how LFMC can be monitored in practice. In these models, the live to dead transition begins when LFMC drops below 120%. The data from this study show that growing season LFMC values <100% only occur when FAW <0.34 and that live to dead transitions occur at these levels of FAW. Thus, these results are at least consistent with the standard fire behavior fuel models, but with a key added benefit—the ability to use in situ FAW monitoring as a surrogate for LFMC. This study provides a first step toward understanding the dynamics of the mechanism of herbaceous live to dead fuel transition in the growing season. FAW might prove an effective indicator for transferring live to dead and is easier to monitor than LFMC, thus FAW could contribute to better dynamic representations of fuel bed parameters in fire danger models.

Conclusion

Two growing seasons of intensive sampling of the temporal dynamics of live fuel moisture content (LFMC), live fuel mass, and dead fuel mass in tallgrass prairie provided new insights into the relationships between fuel bed parameters and soil moisture, expressed as fraction of available water capacity (FAW). LFMC exhibited a nonlinear, threshold-type relationship with FAW, with LFMC being insensitive to FAW at FAW levels above 0.56 and positively related to FAW below that threshold. In addition, this study provides a first step toward understanding the causal mechanism of live to dead fuel transition in the growing season in relation to FAW. Live to dead fuel transitions occurred around a FAW value of 0.34, with the rate of transition increasing approximately linearly as FAW dropped below that threshold.

Prior studies showed that large growing season wildfires in Oklahoma occur primarily when FAW < 0.2 (Krueger et al., 2015) and that the probability of wildfire can increase three-fold as FAW decreases from 0.5 to 0.2 (Krueger et al., 2016). This study provides the missing link between FAW and wildfire behavior, showing that LFMC declines as FAW drops below 0.56 and that live herbaceous fuel transitions to dead fuel

as FAW drops below 0.34. When FAW falls below 0.2, representing extreme drought conditions, grassland LFMC can drop below 100% and live to dead fuel transition can reach rates up to ~18 g m^{-2} d^{-1}.

As soil moisture data become increasingly available due to the development of in situ monitoring networks and of soil moisture satellites, the prospect of using soil moisture data in fire danger assessments becomes increasingly attractive. Estimating LFMC and transferring live fuels to dead based on observed FAW could contribute to better dynamic representations of fuel bed parameters in fire danger models. Improved fire danger ratings could enhance wildfire preparedness and response, which could help reduce the devastating impacts of wildfire on property and lives.

References

Allen, R.G., Pereira, L.S., Raes, D., Smith, M., 1998. Crop evapotranspiration-Guidelines for computing crop water requirements-FAO Irrigation and drainage paper 56. FAO, Rome 300, D05109.

Bradshaw, L.S., Deeming, J.E., Burgan, R.E., Jack, D., 1984. The 1978 national fire-danger rating system: technical documentation.

Carlson, J., Burgan, R., 2003. Review of users' needs in operational fire danger estimation: the Oklahoma example. International Journal of Remote Sensing 24, 1601-1620.

Cheney, N., Gould, J., Catchpole, W.R., 1998. Prediction of fire spread in grasslands. International Journal of Wildland Fire 8, 1-13.

Cheney, P., Sullivan, A., 2008. Grassfires: fuel, weather and fire behaviour. CSIRO PUBLISHING.

Chuvieco, E., Aguado, I., Dimitrakopoulos, A.P., 2004a. Conversion of fuel moisture content values to ignition potential for integrated fire danger assessment. Canadian Journal of Forest Research 34, 2284-2293.

Chuvieco, E., Cocero, D., Martín, P., Martínez, J., De la Riva, J., Pérez, F., 2003. Combining NDVI and surface temperature for the estimation of fuel moisture content in forest fire danger assessment, Fourth International Workshop on Remote Sensing and GIS Applications to Forest Fire Management.

Chuvieco, E., Cocero, D., Riaño, D., Martin, P., Martínez-Vega, J., de la Riva, J., Pérez, F., 2004b. Combining NDVI and surface temperature for the estimation of live fuel moisture content in forest fire danger rating. Remote Sensing of Environment 92, 322-331.

Chuvieco, E., González, I., Verdú, F., Aguado, I., Yebra, M., 2009. Prediction of fire occurrence from live fuel moisture content measurements in a Mediterranean ecosystem. International Journal of Wildland Fire 18, 430-441.

Ellsworth, L., Dale, A., Litton, C., Miura, T., 2017. Improved fuel moisture prediction in non-native tropical Megathyrsus maximus grasslands using Moderate-Resolution Imaging Spectroradiometer (MODIS)-derived vegetation indices. International Journal of Wildland Fire 26, 384-392.

Ford, T.W., McRoberts, D.B., Quiring, S.M., Hall, R.E., 2015. On the utility of in situ soil moisture observations for flash drought early warning in Oklahoma, USA. Geophysical Research Letters 42, 9790-9798.

Gillen, R.L., Tate, K.W., 1993. The constituent differential method for determining live and dead herbage. Journal of Range Management, 142-147.

Hoerling, M., Eischeid, J., Kumar, A., Leung, R., Mariotti, A., Mo, K., Schubert, S., Seager, R., 2014. Causes and predictability of the 2012 Great Plains drought. Bulletin of the American Meteorological Society 95, 269-282.

Krueger, E.S., Ochsner, T.E., Carlson, J., Engle, D.M., Twidwell, D., Fuhlendorf, S.D., 2016. Concurrent and antecedent soil moisture relate positively or negatively to

probability of large wildfires depending on season. International Journal of Wildland Fire 25, 657-668.

Krueger, E.S., Ochsner, T.E., Engle, D.M., Carlson, J., Twidwell, D., Fuhlendorf, S.D., 2015. Soil moisture affects growing-season wildfire size in the southern great plains. Soil Science Society of America Journal 79, 1567-1576.

OSU Extension (2017). *March 7 wildfire impacts in Oklahoma exceed $16 million*. Retrieved from http://www.dasnr.okstate.edu/Members/donald-stotts-40okstate.edu/march-7-wildfire-impacts-in-oklahoma-exceed-16-million.

Ochsner, T.E., Cosh, M.H., Cuenca, R.H., Dorigo, W.A., Draper, C.S., Hagimoto, Y., Kerr, Y.H., Njoku, E.G., Small, E.E., Zreda, M., 2013. State of the art in large-scale soil moisture monitoring. Soil Science Society of America Journal 77, 1888-1919.

Pellizzaro, G., Cesaraccio, C., Duce, P., Ventura, A., Zara, P., 2007. Relationships between seasonal patterns of live fuel moisture and meteorological drought indices for Mediterranean shrubland species. International Journal of Wildland Fire 16, 232-241.

Qi, Y., Dennison, P., Spencer, J., Riaño, D., 2012. Monitoring live fuel moisture using soil moisture and remote sensing proxies. Fire Ecology 8, 71-87.

Scott, J.H., Burgan, R.E., 2005. Standard fire behavior fuel models: a comprehensive set for use with Rothermel's surface fire spread model. The Bark Beetles, Fuels, and Fire Bibliography, 66.

Wang, M., Yang, B., Hu, F., Zang, X., 2014. On-orbit geometric calibration model and its applications for high-resolution optical satellite imagery. Remote Sensing 6, 4391-4408.

Yebra, M., Chuvieco, E., Riaño, D., 2008. Estimation of live fuel moisture content from MODIS images for fire risk assessment. Agricultural and Forest Meteorology 148, 523-536.

Yebra, M., Dennison, P.E., Chuvieco, E., Riaño, D., Zylstra, P., Hunt, E.R., Danson, F.M., Qi, Y., Jurdao, S., 2013. A global review of remote sensing of live fuel moisture content for fire danger assessment: Moving towards operational products. Remote Sensing of Environment 136, 455-468.

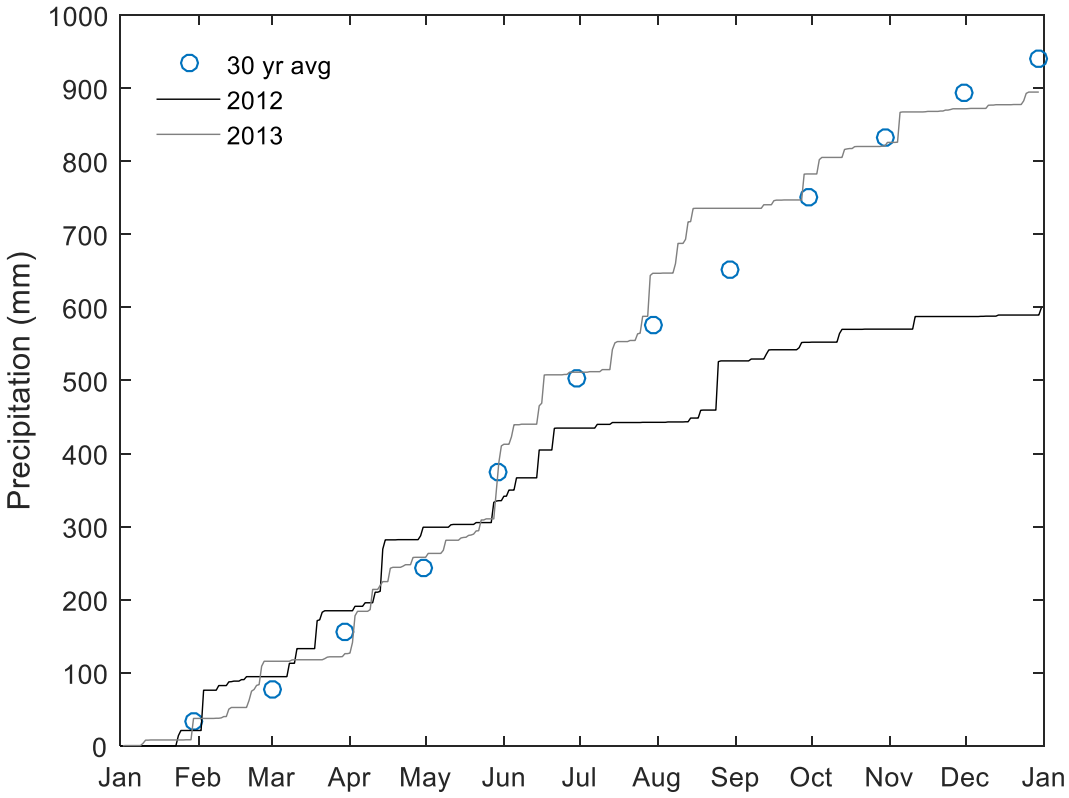

Figure 1: Cumulative precipitation for 2012 and 2013 at the Marena station of the Oklahoma Mesonet along with 30 years average monthly precipitation for the site

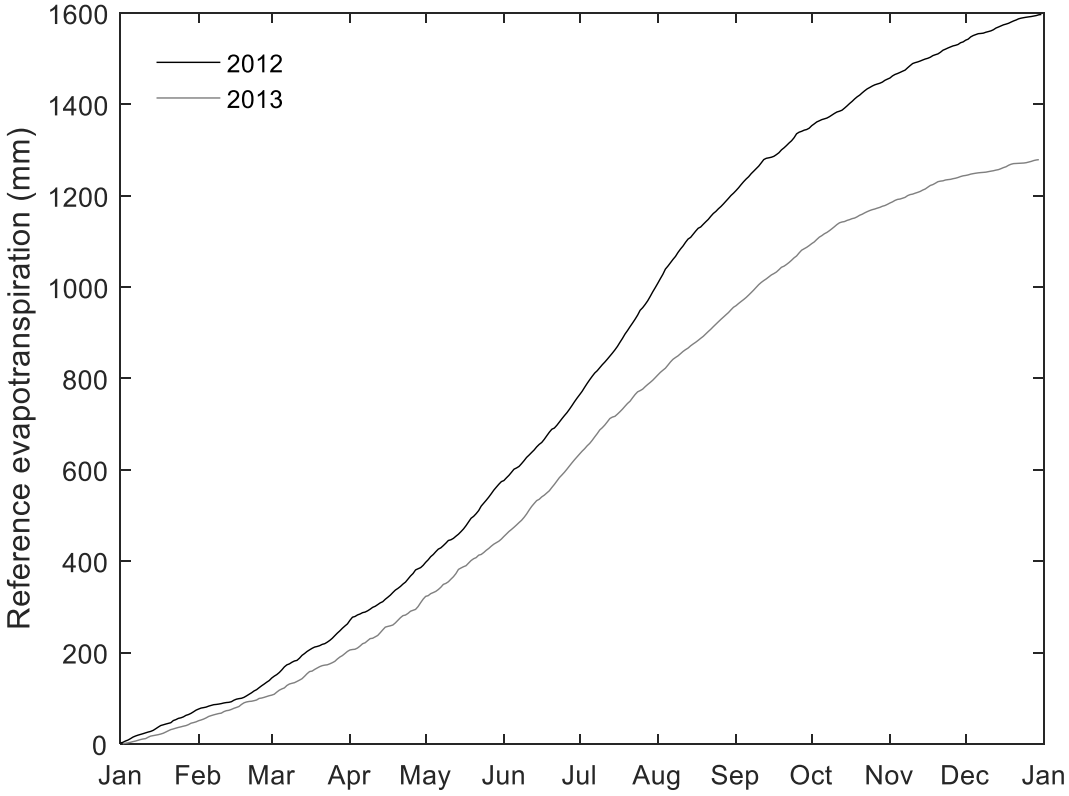

Figure 2: Reference evapotranspiration for 2012 and 2013 at the Marena station of Oklahoma Mesonet

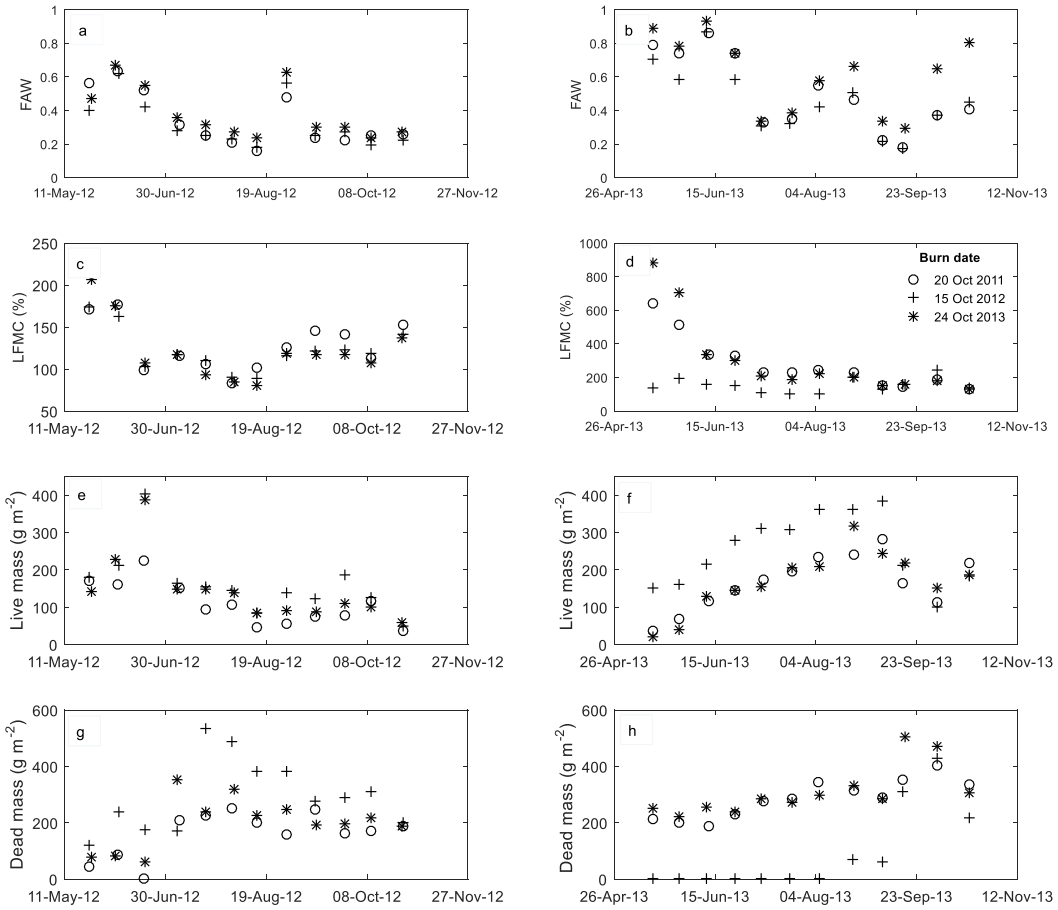

Figure 3: Time series of fraction of available water capacity (FAW) for the 0-40 cm layer, live fuel moisture content (LFMC), live mass, and dead mass, grouped by burn date for the 2012 and 2013 growing seasons. Each data point is the mean across three pastures.

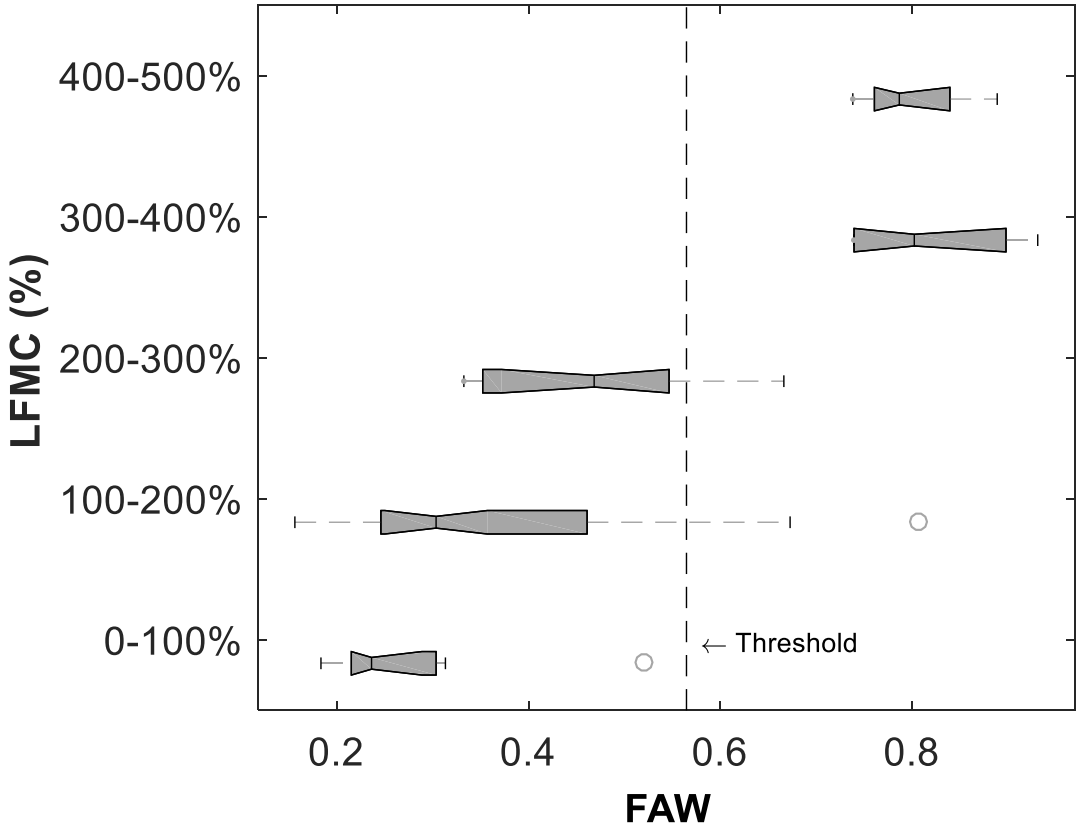

Figure 4: Fraction of available water capacity (FAW) measured for the 0-40 cm soil layer. Live fuel moisture content (LFMC) during the growing season for tallgrass prairie in Oklahoma from 2012-2013 as influenced by soil layer. Median lines are the black lines near the middle of each box, the 25th and 75th percentile values are the left and right sides of boxes, the whiskers indicates the range of data, and the outliers are represented as individual points outside of the whiskers.

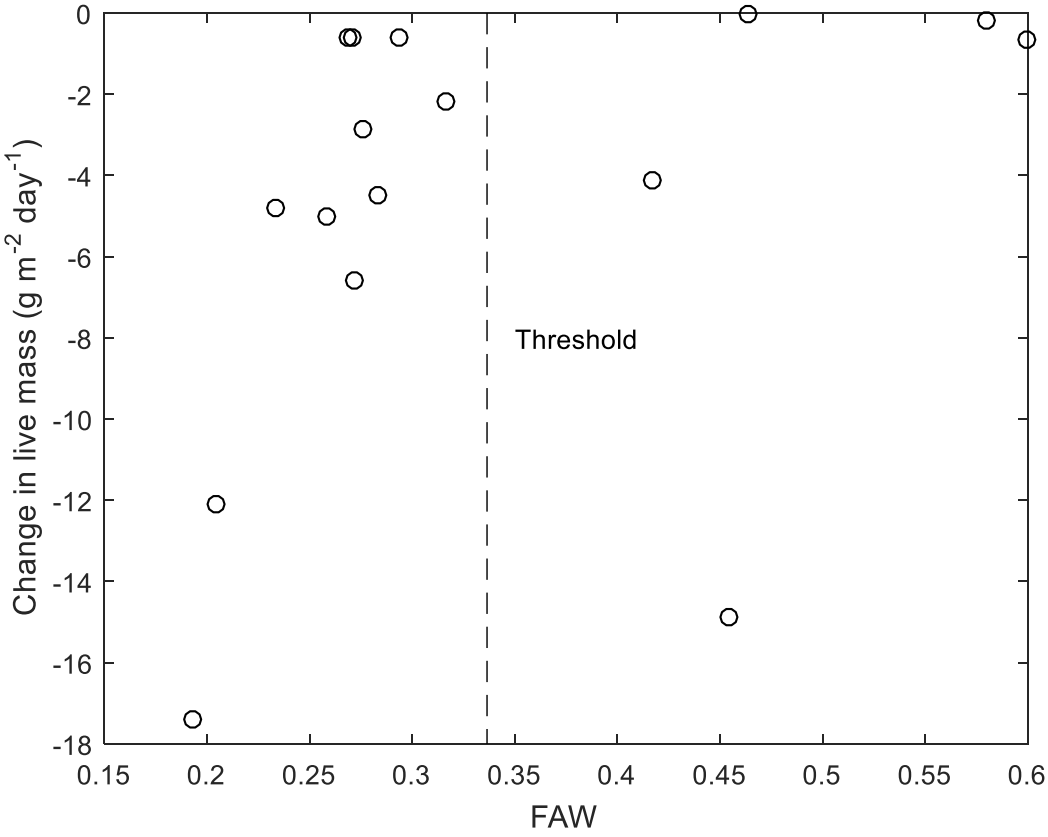

Figure 5: Transitions from live fuel to dead fuel versus fraction of available water capacity (FAW) for the 0-40 cm soil layer.

CHAPTER IV

Preliminary evaluation of a DSSAT model for forage forecasting in Southern Great Plains grasslands

Abstract:

Rangelands are an important part of grassland ecosystems, characterized by high inter-annual variability in precipitation amounts leading to inter-annual variation in forage production that ultimately determines appropriate stocking rates in grazing livestock production. Accurate and timely forecast of forage production several months in advance could be helpful for grazing management, allowing farmers, ranchers, and livestock managers to maintain the sustainability of their operations against adverse conditions such as droughts. Rainfall, soil moisture, and standing crop (measured biomass) have shown potential as predictors of future levels of above-ground biomass in prior studies. Yet, none of the prior studies have resulted in a proven method for in season forage forecasts informed by soil moisture observations. The CROPGRO perennial forage model has been successfully used to simulate growth of tropical guinea grass and palisade grasses in South America but the accuracy of this model in North American tallgrass prairie is unknown. To evaluate the potential use of this model for in season forage forecasting in the US Great Plains, it was necessary to first quantify the model's accuracy using plant parameters taken or adapted from the existing literature. During the growing season of 2012-2013, live mass and soil moisture in form of volumetric water content was measured in tallgrass prairie near

Stillwater, OK. The study spanned nine patches located within three pastures under patch burn management. The uncalibrated forage model was not effective in estimating the average RMSE of live mass but it was reasonably accurate in estimating the average RMSE of soil moisture. In light of this finding, the next step would be using calibrating the model's plant parameters from the observed live mass data to allow improved prediction accuracy from the model.

Introduction

Rangelands span approximately 54% of terrestrial ecosystems and they support 30% of world's population (Sala et al., 2017). In the United States, rangelands occupy 31% of total land area, approximately 308 million ha, mainly in the western US, including the grasslands of the Southern Great Plains (Havstad et al., 2009). These rangelands are characterized by variability in precipitation amounts leading to inter- annual variation in forage production that ultimately determines appropriate stocking rates in grazing livestock production. Accurate and timely forecasts of forage production several months in advance could be helpful for grazing management, allowing farmers, ranchers, and livestock managers to protect rangelands from degradation and to maintain the sustainability of their operations against adverse conditions such as droughts (Don and Woodmansee, 1975; Zhao et al., 2007).

The dynamics of forage production in grasslands are influenced by multiple environmental factors including soil texture, landscape position, land use (fire and grazing), soil fertility, precipitation, and temperature (Alhamad et al., 2007; Andales et al., 2006; Dahl, 1963;

Fuhlendorf and Engle, 2004; Lauenroth and Sala, 1992; Pequeno et al., 2014; Smoliak, 1956; Torell et al., 2011). However, precipitation, more than any other single factor, has been the focus in prior studies. For example, April — July precipitation and biomass production were positively correlated ($r = 0.76$) in native sod of mixed prairie type in Mandan, North Dakota (Rogler and Haas, 1947). May and June precipitation had a strong linear relationship ($r^2 = 0.738$) with biomass production in a shortgrass prairie which included Western wheatgrass (*Agropyron smithii*), Blue gamma (*Bouteloua gracilis*), June grass (*Koeleria cristata*), and needle-and-thread (*Stipa Comata*) in Southeastern Alberta (Smoliak, 1956). Biomass production had a stronger relationship with both seasonal and annual precipitation than with temperature in shortgrass steppe site in north-central Colorado (Lauenroth and Sala, 1992).

However, various studies found that inter-annual variations in biomass production at single site were not adequately explained by annual precipitation alone (Lauenroth and Sala, 1992; Oesterheld et al., 2001). Instead, inter-annual variation in above ground net primary productivity (ANPP) was related to both precipitation in the current year and ANPP of the previous year in shortgrass steppe of Colorado, USA (Oesterheld et al., 2001). One possible mechanism proposed to explain this lag effect included carry-over of water, i.e. soil moisture, from one year to the next and changes in plant community structure, e.g. plant density or leaf area. If these mechanisms are, in fact, significant drivers of inter-annual variations in forage production, then soil moisture data and remotely sensed vegetation indices may have potential for use in forage forecasting.

Soil moisture was found to be a useful predictor of forage production in native mixed prairie in North Dakota (Rogler and Haas, 1947). Stored spring soil moisture was related to seasonal forage production in Eastern Colorado Range Station (Dahl, 1963). In New Mexico, end of season forage production was estimated more effectively using soil moisture measurement instead of seasonal rainfall (Torell et al., 2011). The development of large-scale soil moisture monitoring networks and satellites (Ochsner et al., 2013) has provided the opportunity to use soil moisture data to estimate forage production, but doing so will require the identification or development of models that accurately describe the interactions between soil moisture conditions and forage production.

Models that can utilize soil moisture observations for forage forecasting may be either statistical models or process-based simulation models. For example, a statistical model (Box and Jenkins auto-regressive integrated moving average) informed by available forage measurements and Normalized Difference Vegetation Index data was used to provide 6 weeks forecasts of forage production for three sites in southwestern Texas (Alhamad et al., 2007). Process-based simulation models considered mechanism of crop growth and developmental whereas statistical models do not consider mechanisms of crop parameters such as light extinction coefficient, radiation use efficiency, maximum rooting depth and optimum temperature. The process-based simulation model, Phytomass Growth Model (PHYGROW), has been used to model forage production and availability in Africa (Stuth et al., 2005). The Great Plains Framework for Agricultural Resource Management (GPFARM) forage growth model has been used to forecast

within-season mixed-grass prairie in Wyoming, USA (Andales et al., 2006). These forecast results were then compared to observations from 1983 to 2001, and the model explained 66% of the variability in above-ground biomass (Andales et al., 2006). The GPFARM–Range model was also used to accurately simulate forage growth under different grazing managements in the northern part of the Great Plains (Adiku et al., 2011). And, the ALMANAC (Agricultural Land Management Alternatives with Numerical Assessment Criteria) model has been used to simulate forage production in perennial grass at El Reno, Oklahoma (Kiniry et al., 2013). Yet, none of the studies mentioned above produced in season forage forecasts informed by soil moisture observations.

One of the most extensively developed families of crop growths models is the Decision Support System for Agrotechnology Transfer family of model (DSSAT) (Jones et al., 2003). The DSSAT models include the CROPGRO perennial forage model that was used to simulate forage production of palisade grass (*Brachiaria brizantha*) in state of Sao Paulo, Brazil (Pequeno et al., 2014). The CROPGRO perennial forage model has also been successfully used to simulate growth of tropical guineagrass (Panicum maximum) (Lara et al., 2012), but the accuracy of this model in North American tallgrass prairie is unknown. To evaluate the potential use of this model for in season forage forecasting in the US Great Plains, it was necessary to first quantify the model's accuracy using plant parameters taken or adapted from the existing literature. Thus, the objective of this study was to evaluate the CROPGRO perennial forage model for simulating

forage production and soil moisture in tallgrass prairie using the previously calibrated plant parameters from the literature.

Materials and Method

Study Site

The study site were located in tallgrass prairie at the Oklahoma State University Range Research Station (36.06˚N, -97.21˚E) located near Stillwater, Oklahoma. Major vegetation species were little bluestem (*Schizachyrium scoparium* Michx), big bluestem (*Andropogon gerardii*), Indiangrass (*Sorghastrum nutans*), post oak *(Quercus stellate* Wang), and eastern redcedar (*Juniperus virginiana*). The predominant soils included the Grainola series (fine, mixed, thermic Vertic Haplustalf) covering approximately 60% of the area, and the Coyle series (fine-loamy, siliceous, thermic Udic Argiustoll) covering approximately 35% of the area (Gillen et al., 1990). The study site consisted of three pastures ranging in size from 50–63 ha. Those pastures were sub-divided into six approximately equal sized unfenced patches. These patches were used in a patch burning treatment designed to increase ecological heterogeneity while preventing woody plant encroachment (Fuhlendorf and Engle, 2004). Each year, two of the six patches were burned: one during the late dormant season (February-April) and one during the late growing season (July-October). Patches were burned every three years to represent different successional stages culminating in full recovery for this site after the third year (Fuhlendorf and Engle, 2004). The patch burning sequence has been continuous since the pastures were established in 1999. In the present study, sampling occurred in the patches burned at the end of the growing season. The experimental design was thus a randomized complete block with three treatments, i.e. patches

with three different levels of time since burning, and three replications, i.e. the three pastures (Fuhlendorf and Engle, 2004).

Field Data for Model Evaluation

Aboveground live biomass (g m^{-2}) was measured every two weeks primarily during growing seasons of 2012 and 2013. The growing season was defined as the months of May through October but sampling spanned from March to November. Vegetation samples in twelve randomly selected 0.25 m^2 quadrats were clipped after noon in each of the nine patches during each sampling period. The mixture of live and dead herbaceous material were clipped from each quadrat, collected, weighed, and dried in a 70°C drying oven for 48 h. The percentage of live and dead in each sample was calculated based on the constituent differential method (Gillen and Tate, 1993). This method is based on the difference in moisture content of pure live and pure dead subsamples. Live mass was calculated as the product of the proportion of live in the mix and the dry weight of each quadrat sample.

Soil moisture in form of volumetric water content was measured hourly at four different depths (5, 10, 20 and 50 cm) using reflectometry-based sensors (Model CS655, Campbell Scientific, Logan, UT) in each sampled patch in all three pastures. Those hourly data were averaged to produce daily data. The CS655 soil moisture sensors were calibrated using soil from the Coyle-Lucien complex (36.06142ºN, 97.21727ºW). Soil physical properties required by the model were determined from the soil sampling done on March 13th, 2013. The following soil

properties were measured: i) bulk density, ii) volumetric water content retained at -10, and at -1500 kPa, and iii) percent of sand, silt, and clay. Weather data for the period of 2012-2013 were obtained from the Marena Station of the Oklahoma Mesonet (McPherson et al., 2007), and all three pastures were within 6 km of this station. Weather data included daily maximum and minimum air temperature (˚C), minimum and maximum relative humidity (%), average wind-speed (m s^{-1}), rainfall (mm), and solar radiation (W m^{-2}).

Model parameters and initialization

The DSSAT system is a collection of different crop simulation models that account for the effects of soil, weather and crop management and have been extensively tested with experimental data (Jones et al., 2003). The CROPGRO perennial forage module of DSSAT has been adapted and calibrated for guinea grass (*Panicum maximum*) (Lara et al., 2012), palisade grass (*Brachiaria brizantha* cv. Xares) (Pequeno et al., 2014), and bahiagrass (*Paspalum notatum* Flugge) (Rymph et al., 2004). Plant parameters from Pequeno et al. (2014) were used for this study because little bluestem, the most common grass species at the study site, shares some common features with palisade grass (Table 1). Both have good drought resistance are moderately tolerant of reduced light, are warm season C4 grasses, are perennials with short rhizomes (Forages; Tober and Jensen, 2013). However, little bluestem often reproduces by tillering (NDMC) whereas palisade grass can be propagated vegetatively by sod, stolon's and rhizomes (FAO).

Parameters such as fraction of incoming solar radiation intercepted by leaf canopy and maximum leaf photosynthetic rate were based on published values for light extinction coefficient (k) and radiation use efficiency (RUE) for little bluestem (Kiniry et al., 2002). The fraction of incoming solar radiation intercepted by canopy was calculated following Beer's Law:

$$Fraction = \left(1 - e^{-k*LAI}\right) \qquad [1]$$

where k = 0.36, RUE = 3.4 g MJ^{-1}, LAI = Leaf Area Index = 2.9 . LAI is defined as changes in leaf canopy and it is function of plant density and growing degree days. The fraction of incoming solar radiation when calculated, we obtained = 4.63. RUE is defined as the increase in aboveground dry weight with an increase in unit of photosynthetically active radiation (PAR) and RUE quantifies the biomass production with an assumption of sufficient nutrient management. The maximum leaf photosynthetic rate (LF_{MAX}) was calculated using the canopy model as adapted from Boote and Jones (1987).

$$LF\max = PG_C * \frac{1}{k}\left(1 - e^{-k(LAI)}\right) * RUE \qquad [2]$$

where PG_c = amount of photosynthetically active radiation hitting the leaf and it is assumed to be 2000 J m^{-2} s^{-1}, and LF_{max} is the maximum value (mg CO_2 m^{-2} s^{-1}), and RUE = 3.4 g MJ^{-1}. Using Eq [2], we obtained LF_{max} = 1.48 mg CO_2 m^{-2} s^{-1} (Table 1). In addition, a base temperature of 12˚C, optimum temperature of 25.8˚C and thermal units to reach maturity was 1800 degree days

as taken from Kiniry et al. (2002). The photoperiod requirement for plant growth, culm elongation, and flower elongation for little bluestem was taken as 13-15 h (Phan, 2000).

Soil data from the nine patches was imported in DSSAT and a .soil file with multiple soil profiles was created. Initial plant weights as measured on the first sampling date in each growing season were used to initialize the conditions of each patch. In addition, to account for the effects of grazing, the amount of biomass consumed by livestock on an animal unit (AU) basis was estimated to be 12 kg AU^{-1} d^{-1} and forage disappearance was estimated at 12 kg AU^{-1} d^{-1}. Disappearance of biomass could be due to trampling effects and biomass eaten by other animals or insects rather than livestock animals. The stocking rate, in terms of animal units (AU), was calculated based on average weight of the cows, average calving dates and weaning weights for each pasture:

$$Stocking\,rate = \frac{1\ cow/calf\ pair}{6.87\ ha} \quad [3]$$

$$(Cow\ AU) = \frac{weight\ of\ cow - 100}{1000} = \frac{1155 - 100}{1000} = 1.05 \quad [4]$$

$$(Calf\ AU) = \frac{weight\ of\ calf + 100}{1000} = \frac{75 + 100}{1000} = 0.175 \quad [5]$$

Therefore, the combined consumption and disappearance of biomass based on equation 3, 4 and 5 was estimated at 4.30 kg ha^{-1} d^{-1} but due to an error in calculation, for the simulation for live mass in this dissertation, we used the value of 9.84 kg ha^{-1} d^{-1}. Grazing was represented in

the model by removing the total value of consumption and disappearance of biomass from the leaf and stem state variables in the model on a daily basis. The value of 9.84 kg/ha/day was constant for each patch. For initializing soil moisture, the measured values at four different depths (5, 10, 20 and 50 cm) for each patch on the first vegetation sampling date of each season were used. There were some missing values in the soil moisture data, so we used two approaches: i) for missing data at 20 cm, we used a multiple linear regression model with 10 and 50 cm data as independent variables and 20 cm as the dependent variable and ii) for missing data at 50 cm in one patch, we used 50 cm data from the remaining two patches in the same pasture and 20 cm data from the same patch in multiple linear regression models.

Initialization of values

The aboveground biomass and belowground biomass at the start of each season were initialized by setting the MOW parameter in the .GOT file. For initializing, we used the initial aboveground biomass measured in each patch during the first sampling event of each year. The MOW parameter is defined as the amount of stubble remaining after harvest in the prior year and includes the above and below-ground biomass. For belowground biomass, we estimated the initial belowground biomass based on biomass of the rhizomes, and upper and lower roots measured for big bluestem in tallgrass prairie in Kansas (Hayes, 1986). These estimated values were constant for each location. We simulated that there is no effect of nitrogen on our study. Soil organic matter was modeled using the Parton model from the Century-SOM module (Parton et al., 1987).

Parameterization of values

The CROPGRO forage model adapted for palisade grass was used in our study (Pequeno et al., 2014). We adjusted some parameters including the maximum leaf photosynthetic rate, base temperature, and first optimum temperature based on values for little bluestem from Kiniry et al. (2002). We did not modify the growth partitioning parameters (YLEAF, YSTEM and YSTOR values) from Pequeno et al. (2014). The MVS parameter (hypothetical number of leaves left on a primary tiller axis after harvest) was defined in the MOW file and was set at 2. Similarly, the temperature have effects on leaf area expansion and internode elongation resulting in change in specific leaf area (SLA). The base temperature that affects SLA was kept at 10.3˚C and optimum temperature of 24.2˚C when expansion occurred at optimum rate. The optimized value for specific leaf area of cultivar was taken as 190 cm^2 g^{-1} under standard growth conditions with optimum temperature, water and high light for early vegetative phase. The specific leaf areas representing the thinnest and thickest leaves under low and high light respectively were set to 340 and 139 cm^2 g^{-1}.

Statistical evaluation of model performance

Simulated live mass and soil moisture were compared with measured live mass and soil moisture. For evaluating model performance, we used root mean square error (RMSE), coefficient of determination (R^2), the ratio of measured and simulated data, and the Willmott agreement index (d-statistic) (Willmott et al., 1985). RMSE is calculated as:

$$RMSE = \sqrt{\frac{1}{N}\sum_{i=1}^{N}\left(Y_i - \hat{Y}_i\right)^2} \qquad [6]$$

where N is the total number of observations, Y_i is observed value while $\hat{Y}_i$ is predicted value simulated by model. Better models have smaller RMSE values. The Willmott agreement index is calculated as follows:

$$d = 1 - \left[\frac{\sum_{i=1}^{N}(Y_i - \hat{Y}_i)^2}{\sum_{i=1}^{N}\left(\left|\hat{Y}_i - \bar{Y}\right| + \left|Y_i - \bar{Y}\right|\right)^2}\right], \qquad [7]$$

where N is the total number of observations, Y_i is measured data while $\hat{Y}$ is the simulated value and $\bar{Y}$ is the mean of the measured data. A d index near one represents a good model.

Results

Precipitation patterns

The cumulative precipitation was approximately 50 mm above average by end of April 2012, creating favorable conditions for early season vegetative growth as seen in Fig 1. However, below average rainfall in end of May 2012 resulted in cumulative precipitation falling below average. There was an increase in precipitation deficit in the months of June and July and the deficit reached approximately 150 mm by end of July. There was some precipitation in the middle of August of 2012 but by end of 2012, the cumulative precipitation was approximately

300 mm below average. Whereas, the cumulative precipitation was near or above average over throughout (Fig. 1).

Simulation of live mass and comparison with observed live mass

In 2012, there was high live mass at the beginning of growing season for all the patches (Fig 2). The observed live mass peaked to as high as 6000 kg ha^{-1} on 5th and 19th July, 2012. The simulated live mass for 2012 ranged from 0–5000 kg ha^{-1} (Fig. 2), with most of the locations within 0–4000 kg ha^{-1}. The simulated model worked well in response of the difference between simulated and measured live mass for all the locations except for patch 1 of Pasture 9 and 17, where the simulated model overestimated the live mass by approximately 1000 kg ha^{-1} (Fig 2). The simulation model explained approximately 0.6 proportional differences in the observed and simulated means and variance (Willmott's $d > 0.6$) for pasture 5 with an exception of patch 5 for 2012, which explained only 0.35 proportional difference in the observed and simulated means and variance (Table 2). The model explained at least 0.3 of difference between measured and simulated data in reference to Willmott's d values and d- index of 0.3 suggested that it had poor agreement in the model for most of the patches. If we compared the ratio of observed and simulated, the model overestimated live mass (Table 2). In most of the forage model, the ratio of observed to simulated values were taken in consideration for evaluating the performance of model.

In 2013, there was steady increase of measured live mass through the growing season, it peaked in the latter part of growing season. The measured live mass reached as high as ~ 8000

kg ha^{-1} on September 15, 2013 with the range from 0–6000 kg ha^{-1} for most of the locations. The simulation model performed better for live mass compared to year 2012 (Fig 3). The range of the simulated live mass was 0–6000 kg ha^{-1} for all the patches. The simulated model was better in 2013 than in 2012 at explaining the variability of live mass for pasture 9 and 5 (Table 2) as shown by the higher Willmott's d values. For pasture 17, the model performed fairly poor for both years ($d < 0.6$). If we compared the ratio of observed and simulated live mass, the model was relatively unbiased for patch 1 and 3 of Pasture 5 (~ 1:1 ratio), but for other patches, it overestimated live mass (Table 2).

Soil Moisture Dynamics

During 2012, near surface, i.e. 5 cm, soil moisture reached maximum values around 0.30 cm^3 cm^{-3} or less in most patches for the early part of growing season (Fig. 4). A fairly extreme 2-month dry period began in mid-June, and soil moisture levels dropped to 0.10 cm^3 cm^{-3} or less by mid-August. We saw the similar dynamics for simulated soil moisture (Fig 4). Most of the time in 2012, the model underestimated soil moisture. The model explained at least 0.7 of difference between measured and simulated data (Willmott et al., 2012) for all the locations in 2012 (Table 3) in reference to Willmott's d values. As far as ratio of observed and simulated soil moisture, we found that both simulated and observed soil moisture are mostly on ~1:1 ratio. We also saw the similar dynamics for other depth (10-20 cm, 20-50 cm, and >50 cm) as shown in Appendix (Fig. 1, 3 and 5 of CHAPTER IV).

We observed the soil moisture as high as 0.4 cm^3 cm^{-3} in the early and middle part of growing season of 2013 while for simulated soil moisture, it was high as 0.5 for 2013 in the early and middle part of growing season (Fig. 5) while for 2012, the soil moisture reached maximum values of 0.3 cm^3 cm^{-3} on the surface. The soil moisture dropped to as low as 0.1 cm^3 cm^{-3} during September and October of 2013. The simulated model underestimated soil moisture in most of the locations (Fig. 5), expect the seasonal trends are mostly as expected. The model explained at least more than 0.8 of difference between simulated and observed data and model with d-index near one indicates a good model prediction. The wetting and drying effects were same for simulated and measured soil moisture for other depth (10, 20, and 50 cm) for 2013 as shown in Appendix (Fig. 2, 4 and 6 of CHAPTER IV). The RMSE for soil moisture was less than 0.03 cm^3 cm^{-3} for most of the locations. Similarly, the ratio of observed and simulated soil moisture were almost ~ 1: 1 (Table 3).

Discussion

The drought conditions which developed starting in late June of 2012 resulted in the decline in both measured and simulated live biomass (Fig. 2). The severe drought in 2012 could have decreased the accuracy of the predictions of live mass due to incomplete representation of drought effects. Similar difficulties have been observed in related studies. For example, there was under prediction of peak standing crop in Wyoming, USA in 2000 due to severe drought using GPFARM forage growth model (Andales et al., 2006). The model also could not simulate late-season recovery of vegetation in the drought year 2001.

Another potential deficiency in the simulations is that they do not account for the prescribed fire treatment and its potential effects on live mass. The transient maxima hypothesis states that periodic fires due to increased light availability and nutrient availability (Blair, 1997) can enhanced aboveground net primary productivity. Therefore, the prescribed fire treatment might have influenced live mass in our study through alterations of light and nutrient availability that were not represented in the model. Grass growth is sensitive to day lengths (Marousky et al., 1992), and the 14 h photoperiod adapted for our study might not be optimal. Furthermore, correctly predicting the impacts of grazing on live mass is complicated by uncertainties about consumption rates and selective grazing influenced by the patch burn management (Fuhlendorf and Engle, 2004). In addition, we have not accounted for the shading effects caused by standing dead biomass and the effects of nitrogen in the study area.

Cumulative precipitation was near or above average throughout 2013, and the model performed slightly better in 2013 for most of the locations compared 2012, as evidenced by the Willmott's d values. But, still the accuracy of the biomass estimation was relatively poor ($d < 0.75$) compared to prior studies in which the model was calibrated for a particular grass species. The CROPGRO model was able to simulate biomass for palisade grass in Piracicaba, Brazil for 2005- 2008 with Willmot's $d = 0.83$ (Pedreira et al., 2011).The CROPGRO model was able to simulated biomass for guinea grass at the same study site from 2003 to 2004 with d of 0.98 (Lara et al., 2012). The same model adapted for Xaraes cultivar of palisade grass improved the simulation of biomass for both irrigated and rainfed conditions at the same study sites from 2011

to 2013 with d of greater than 0.90 (Pequeno et al., 2014). Improved agreement for tallgrass prairie could likely to be attained if we calibrated the model parameters using the observed live mass data.

The model effectively simulated soil moisture with the d index for the 5 cm depth typically greater than 0.8 (Table 3). There is better performance in 2013 than 2012 as we also saw for live mass. The better performance of the model for simulating soil moisture than for live mass could be related to the fact that the soil properties were measured for each location whereas there was no site-specific calibration done for any of the plant parameters. The CERES-Maize model of DSSAT v 3.5 was used to simulate soil moisture content in the central region of Thailand for 1999 and 2000 and both simulated and observed soil moisture showed similar variation with depth and time although that study did not provide the statistical measure for comparing for simulated and observed soil moisture data. The simulated soil moisture were within the 95% confidence interval of the observed data (Asadi and Clemente, 2003). In southwestern Ontario, DSSAT v. 4.5 simulated the soil water content for 2000 under free tile drainage and controlled tile drainage with sub-irrigation with d index of 0.72 and 0.74 respectively for depth of 0–30 cm, while for 2001, it was 0.73 for free tile drainage and 0.83 for controlled tile drainage in corn and soybean (Liu et al., 2011). This result from the study at Ontario is consistent with our study suggesting that the DSSAT models accurately simulate soil moisture.

Conclusion

The results of this study suggest that improved plant and grazing parameters will be needed in order for the CROPGRO perennial forage model to be useful for near time forecasting of forage production in rangeland. The next step to enhance this simulation model would be calibrating the model with the measured live mass data from 2012-2013 and then using additional site-years of data to validate the predictions of potential forage production for the growing season. The *B. brizantha* version of CROPGRO perennial forage model, although adapted for little bluestem, did not accurately simulate the live mass for tallgrass prairie in this study. The severe drought and uncertainties about consumption rates and selective grazing influenced by the patch burn management could have complicated live mass estimation. Though the CROPGRO perennial forage model has proven useful in simulating forage production in study sites in South America, the model requires further parameterization to effectively simulate forage production in tallgrass prairie in Southern Great Plains of the United States. The results from simulation of soil moisture data suggest that the CROPGRO perennial forage model accurately described soil moisture dynamics. We recommend further improvement of plant and grazing parameters based on the observed live mass data collected in this study to facilitate improved forage predictions in tallgrass prairie.

REFERENCES

Adiku, S.G.K., Ahuja, L.R., Dunn, G.H., Derner, J.D., Andales, A.A, Garcia, L., and Bartling, P.N.S. (2011). Parameterization of the GPFARM-Range Model for simulating rangeland productivity. Methods of Introducing System Models into Agricultural Research, 209-228.

Alhamad, M. N., Stuth, J., & Vannucci, M. (2007). Biophysical modelling and NDVI time series to project near- term forage supply: spectral analysis aided by wavelet denoising and ARIMA modelling. International Journal of Remote Sensing, 28(11), 2513-2548.

Andales, A. A., Derner, J. D., Ahuja, L. R., & Hart, R. H. (2006). Strategic and tactical prediction of forage production in northern mixed-grass prairie. Rangeland Ecology & Management, 59(6), 576-584.

Blair, J. M. (1997). Fire, N availability, and plant response in grasslands: a test of the transient maxima hypothesis. Ecology, 78(8), 2359-2368.

Dahl, B. E. (1963). Soil Moisture as a Predictive Index to Forage Yield for the Sandhills Range Type. Journal of Range Management, 16(3), 128-132. doi: 10.2307/3895105

Fuhlendorf, S. D., & Engle, D.M. (2004). Application of the fire–grazing interaction to restore a shifting mosaic on tallgrass prairie. Journal of Applied Ecology, 41(4), 604-614.

Gillen, R. L., McCollum, F. T., Brummer, J. E. (1990). Tiller defoliation patterns under short duration grazing in tallgrass prairie. Journal of Range Management, 95-99.

Havstad, K., P., D., Allen-Diaz, B., Bartolome, J., Bestelmeyer, B., Briske, D.,, Huntsinger, L. (2009). The Western United States rangelands, a major resource. Grasslands: Quietness and Strength for a New American Agriculture. Soil Science Society of America: Madison, WI, USA, 75-93.

Hayes, D. C. (1986). Seasonal root biomass and nitrogen dynamics of big bluestem (Andropogon gerardii Vitman) under wet and dry conditions: Kansas State Univ., Manhattan (USA).

Hoogenboom, G. (2000). Contribution of agrometeorology to the simulation of crop production and its applications. Agricultural and forest meteorology, 103(1), 137-157.

Jones, J. W., Hoogenboom, G., Porter, C. H., Boote, K. J., Batchelor, W. D., Hunt, L.A., Ritchie, J. T. (2003). The DSSAT cropping system model. European journal of agronomy, 18(3), 235-265.

Kiniry, J. R., Johnson, M. V. V., Venuto, B. C., & Burson, B. L. (2013). Novel application of ALMANAC: Modelling a functional group, exotic warm-season perennial grasses. American Journal of Experimental Agriculture, 3(3), 631.

Kiniry, J.R., Sanchez, H., Greenwade, J., Seidensticker, E., Bell, J.R., Pringle, F., Rives, J. (2002). Simulating grass productivity on diverse range sites in Texas. Journal of soil and water conservation, 57(3), 144-150.

McKeon, G. M., & Howden, S.M. (1992). Adapting grazing management to climate change and seasonal forecasting. Paper presented at the Proceedings of the 7th Biennial Conference of the Australian Rangeland Conference. Cobar, NSW.

Ochsner, T. E., Cosh, M. H., Cuenca, R. H., Dorigo, W. A., Draper, C. S., Hagimoto, Y. ,& Zreda, M. (2013). State of the art in large-scale soil moisture monitoring. Soil Science Society of America Journal, 77(6), 1888-1919.

Pequeno, D. N. L., Pedreira, C. G. S., & Boote, K. J. (2014). Simulating forage production of Marandu palisade grass (Brachiaria brizantha) with the CROPGRO-Perennial Forage model. Crop and Pasture Science, 65(12), 1335-1348.

Phan, A. T. (2000). Genetic diversity of blue grama, Bouteloua gracilis, and little bluestem, Schizachyrium scoparium, as affected by selection.

Rogler, G. A., & Haas, H. J. (1947). Range production as related to soil moisture and precipitation on the Northern Great Plains. J. Amer. Soc. Agron, 39, 378-389.

Rymph, S. J., Boote, K. J., Irmak, A., Mislevy, P., & Evers, G.W. (2004). Adapting the CROPGRO model to predict growth and composition of tropical grasses: developing physiological parameters. Paper presented at the Proceedings.

Sala, O. E., Yahdjian, L., Havstad, K., & Aguiar, M. R. (2017). Rangeland Ecosystem Services: Nature's Supply and Humans' Demand Rangeland Systems (pp. 467-489): Springer.

Seligman, N. G., & Keulen, H. V. (1980). 4.10 PAPRAN: A simulation model of annual pasture production limited by rainfall and nitrogen. Simulation of nitrogen behaviour of soil-plant systems, 192.

Stuth, J. W., Angerer, J., Kaitho, R., Jama, A., & Marambii, R. (2005). Livestock early warning system for Africa rangelands. Monitoring and predicting agricultural drought: a global study, 283-296.

Torell, L. A., McDaniel, K. C., & Koren, V. (2011). Estimating Grass Yield on Blue Grama Range From Seasonal Rainfall and Soil Moisture Measurements. Rangeland Ecology & Management, 64(1), 56-66. doi: 10.2111/REM-D-09-00107.1

Willmott, C. J., Ackleson, S. G., Davis, R. E., Feddema, J. J., Klink, K. M., Legates, D. R., Rowe, C. M. (1985). Statistics for the evaluation and comparison of models. Journal of Geophysical Research: Oceans, 90(C5), 8995-9005.

Table 1: Model parameter names, definition, values for base and optimum temperatures, photoperiod effects on vegetative partitioning, and maximum leaf photosynthetic rate for our study.

Name	Definition	Values	Source
PRO_ _ G	'Normal growth' protein conc ; fraction of tissue (leaf, LF; root, RT; stem, ST; storage organ, SR)	LF = 0.16, RT = 0. 04, ST = 0.08, SR = 0.092	(Pequeno et al., 2014)
PRO_ _ I	'Maximum protein concentration of tissue	LF = 0.24, RT = 0.101, ST = 0.12, SR = 0.092	(Pequeno et al., 2014)
PRO _ _ F	'Final' protein concentration of tissue (at senescence)	LF = 0.035 , RT = 0.022, ST = 0.025 , SR = 0.056	(Pequeno et al., 2014)
Tb	Base temperature for vegetation development (˚C)	12.0	(Kiniry et al., 2002)
T01	First optimum temperature for vegetative development (˚C)	25.8	(Kiniry et al., 2002)
T02	Second optimum temperature for vegetative development (˚C)	40.0	(Kiniry et al., 2002)
TM	Maximum temperature for vegetative development (˚ C)	45.0	(Kiniry et al., 2002)
LFMAX	Maximum leaf photosynthetic rate at 30 ˚C, 350 ppm CO_2, and high light	1.48	Calculated

Table 2: Summary statistics for simulated and observed live mass from 2012-2013 in Stillwater, Oklahoma

Pasture-Patch	Year	RMSE (kg $ha^{-1`}$)	R^2	Ratio (obs. /sim.)	Willmot's d
5-1	2012	1579	0.47	0.37	0.58
	2013	1762	0.21	0.99	0.63
5-3	2012	1243	0.36	0.67	0.60
	2013	2143	0.12	0.96	0.58
5-5	2012	1924.	0.38	0.37	0.51
	2013	1936	0.40	0.73	0.68
9-1	2012	2468	0.30	0.22	0.32
	2013	1819	0.41	0.62	0.63
9-3	2012	2169	0.14	0.44	0.44
	2013	2189.5	0.44	0.63	0.67
9-5	2012	806.8	0.52	0.55	0.73
	2013	1092.4	0.44	0.51	0.73
17-1	2012	2714	0.38	0.22	0.35
	2013	3178.9	0.20	0.61	0.43
17-3	2012	1276.1	0.10	0.72	0.51
	2013	3097.0	0.12	0.53	0.36
17-5	2012	1691.7	0.30	0.46	0.55
	2013	2782.2	0.40	0.56	0.55
	Average	1760	0.34	0.56	0.59

Table 3*:* Summary statistics for simulated and observed soil moisture at 5 cm from 2012-2013 in OK

Pasture-Patch	Year	RMSE (cm^3 cm^{-3})	R^2	Ratio (obs. /sim.)	Willmot's d
5-1	2012	0.03	0.65	0.96	0.89
	2013	0.06	0.66	0.87	0.83
5-3	2012	0.04	0.61	0.83	0.80
	2013	0.04	0.73	0.94	0.92
5-5	2012	0.04	0.65	0.88	0.81
	2013	0.05	0.62	0.94	0.85
9-1	2012	0.05	0.5	0.81	0.68
	2013	0.07	0.59	0.78	0.78
9-3	2012	0.05	0.33	1.31	0.68
	2013	0.07	0.56	0.79	0.79
9-5	2012	0.02	0.57	1.02	0.86
	2013	0.04	0.54	0.84	0.84
17-1	2012	0.03	0.64	1.21	0.85
	2013	0.04	0.65	1.09	0.88
17-3	2012	0.04	0.51	0.77	0.74
	2013	0.04	0.6	0.83	0.82
17-5	2012	0.03	0.69	1.14	0.88
	2013	0.05	0.62	1.09	0.88
	Average	0.04	0.58	0.91	0.81

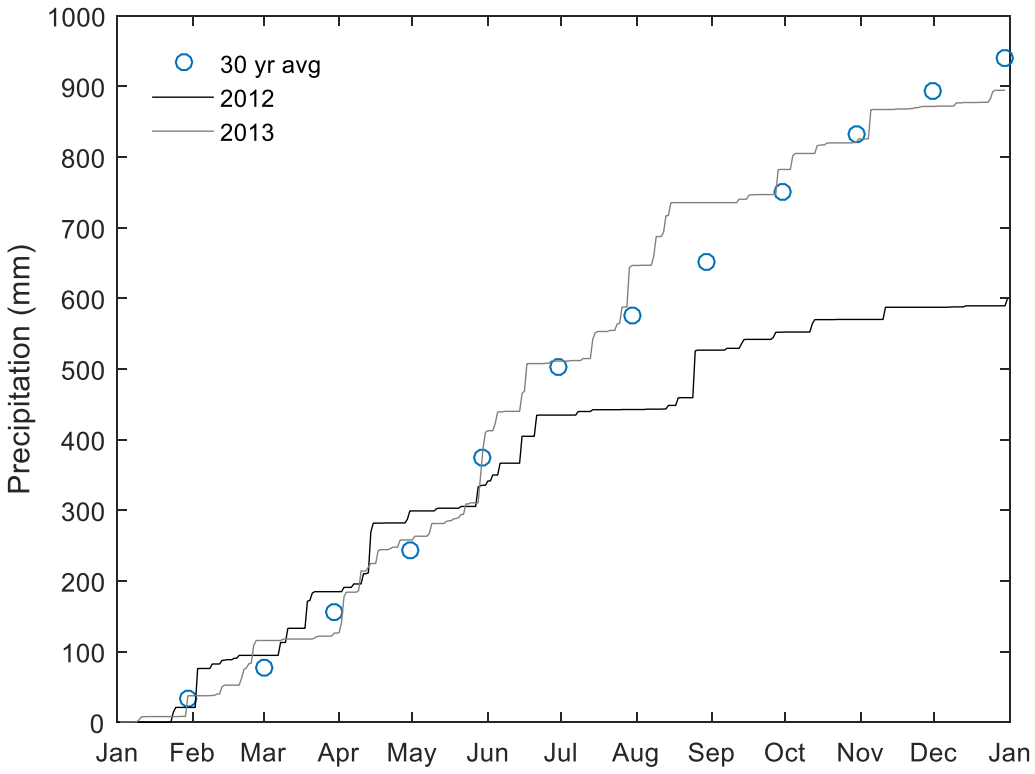

Fig. 1: Cumulative precipitation for 2012 and 2013 at the Marena station of Oklahoma Mesonet along with 30 year average monthly precipitation for the site

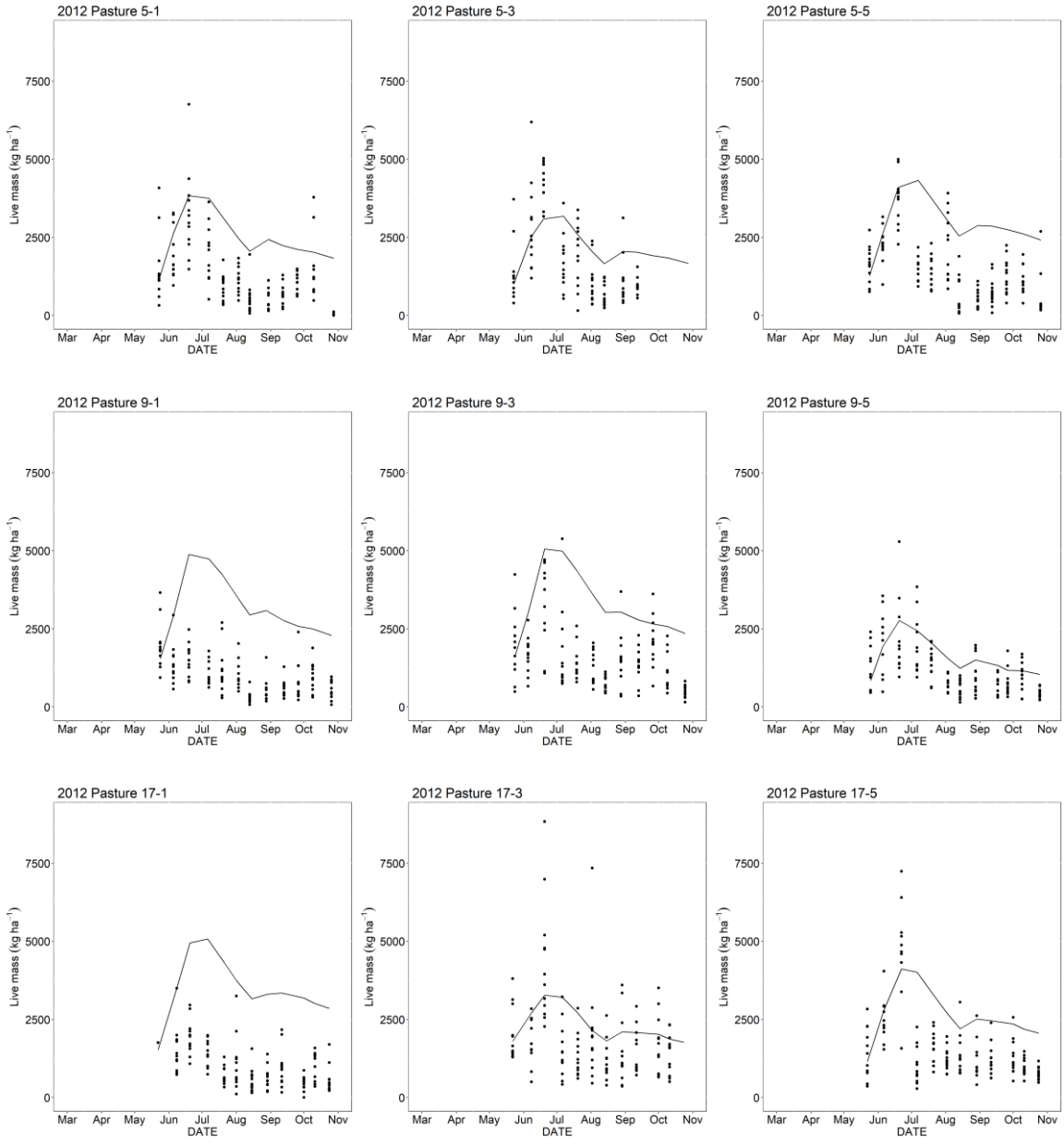

Fig. 2: Simulated and observed live mass (g m^{-2}) for year 2012 at the tallgrass prairie in Stillwater, Oklahoma for each patch of each pasture. The black line represents the simulated live biomass and black dot represents the measured live mass.

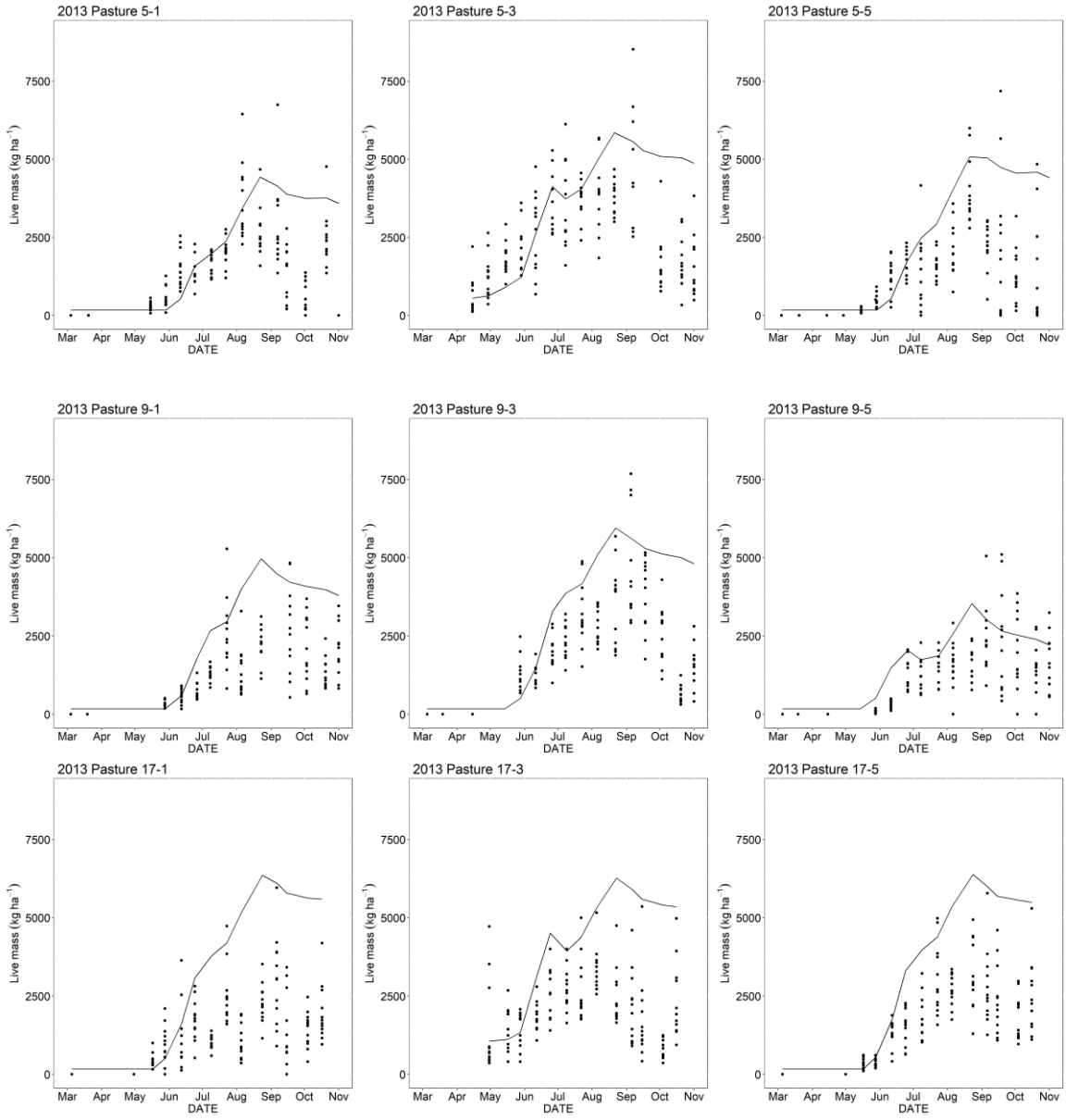

Fig. 3: Simulated and observed live mass (g m^{-2}) for year 2013 at the tallgrass prairie in Stillwater, Oklahoma for each patch of each pasture. The black line represents the simulated live biomass and black dot represents the measured live mass

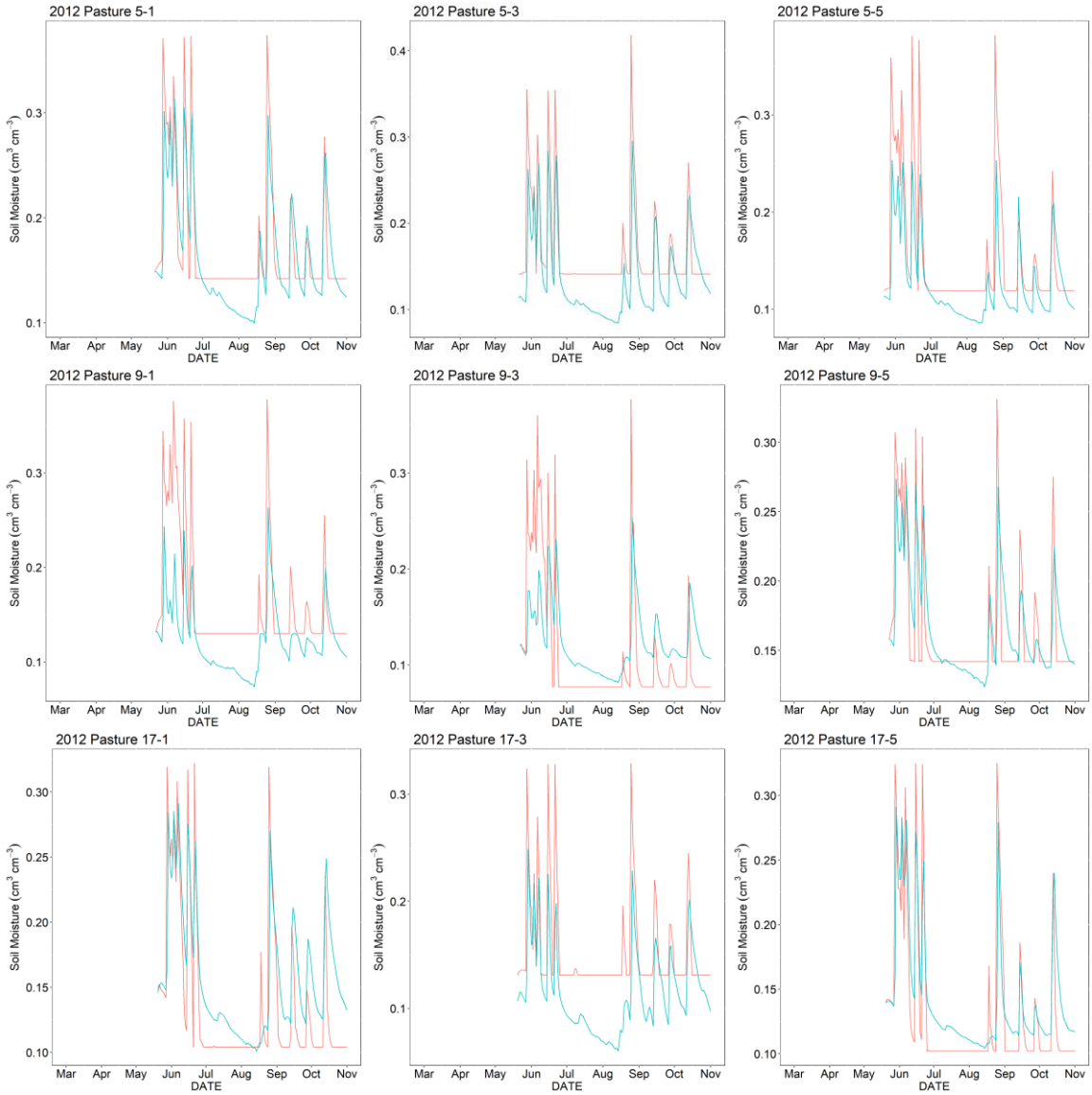

Fig. 4: Simulated and observed soil moisture for year 2012 at the tallgrass prairie in Stillwater, Oklahoma. The red line represents the simulated soil moisture whereas blue color represents the measured soil moisture

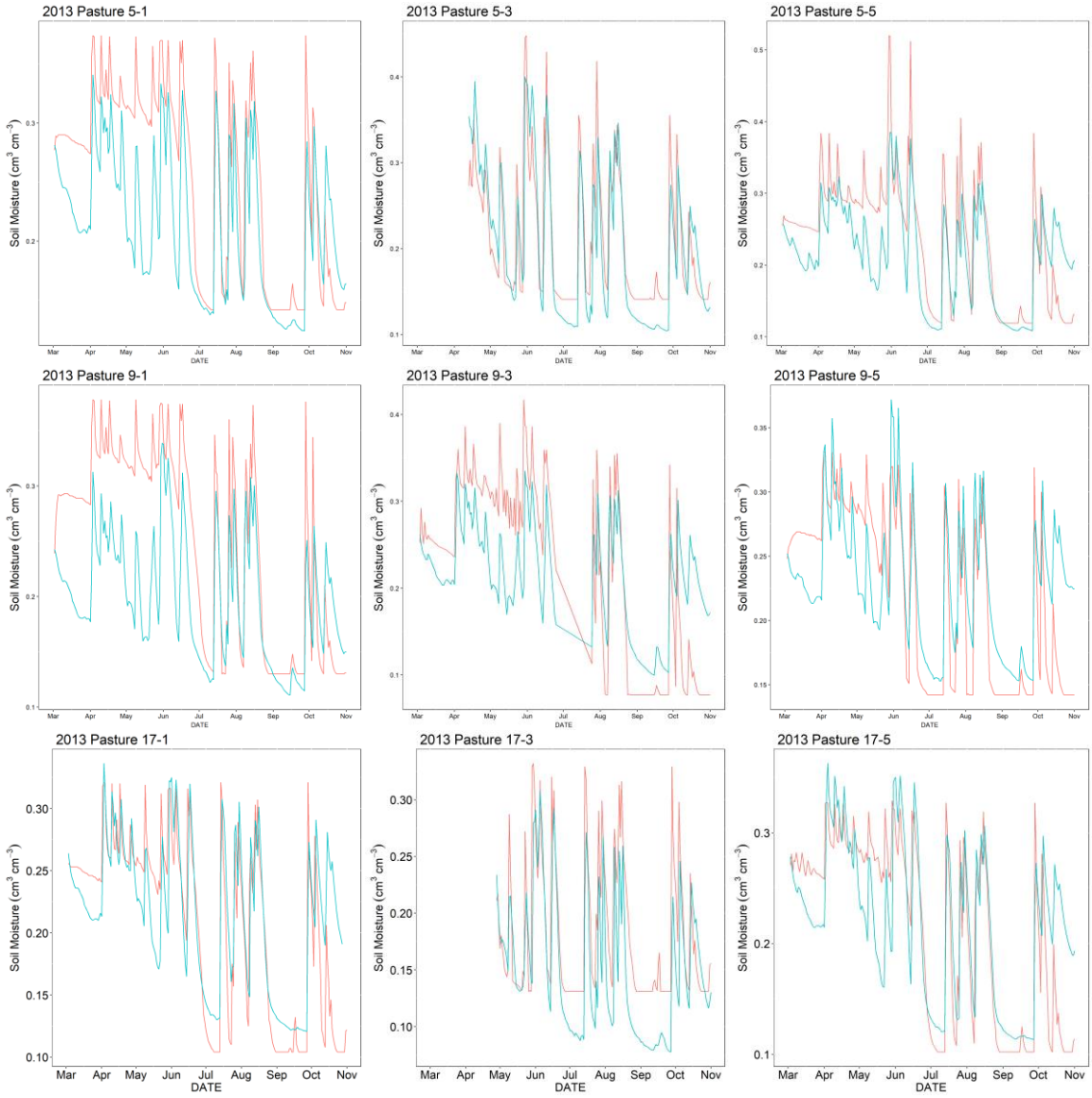

Fig. 5: Simulated and observed soil moisture for year 2013 at the tallgrass prairie in Stillwater, Oklahoma. The red line represents the simulated soil moisture whereas blue color represents the measured soil moisture

CHAPTER V

GENERAL CONCLUSION

Grasslands and grazing systems are essential to agricultural communities in the United States Southern Great Plains (SGP) and in similar climatic regions around the world. In the SGP states of Kansas, Oklahoma, and Texas, cattle and calf production added about $100 billion to the economy in 2011. Additionally, hay production in 2011 was 10 million Mg which added another $1 billion to the region's economy. The SGP contains 55 million ha of total pasture area, including permanent pasture, and cropland used for pasture and pasture woodland. Of that 55 million ha, 9 million ha of pasture are located in Oklahoma (NASS-USDA, 2012). Wise management of these grasslands and grazing systems is necessary not only for economic reasons, but also to conserve soil, protect water quality, and maintain ecosystem services (Belsky et al., 1999; Follett and Reed, 2010; Worrall et al., 2007). However, grassland management in the SGP is challenging because the variable climate creates large uncertainties regarding the vegetat ion productivity both within and between seasons.

In our first study, we examined the potentials of estimating aboveground biomass and fuel moisture content in tallgrass prairie and the study revealed that both the SMLR and ANN models used in our study effectively estimated seasonal changes in above-ground biomass (AGB) and fuel moisture content (FMC). The models, developed from DOY, CH, NDVI, and percent reflectance in five bands, were able to estimate AGB and FMC for tallgrass prairie in Oklahoma with accuracy comparable to that observed in similar studies at other grassland sites. ANN proved better in estimating FMC than SMLR, while for AGB, ANN did not result in substantialy improved estimates in the validation set for our study area. Both types of models underestimated AGB for levels above 600 g m^{-2} and underestimated FMC for levels above 150%. Despite these limitations, the models developed here have been validated using data spanning nine large patches with different burn histories across three different pastures in two years with distinctly different growing conditions. Given this relatively large variance in the underlying datasets, these models should be useful for nondestructive estimation of AGB and FMC in other similar grassland environments, particularly when monitoring large, heterogenous areas for grazing management or wildfire preparedness.

The second study described live fuel moisture content (LFMC) and live to dead transition as function of soil moisture and we found out that temporal dynamics of LFMC, live fuel mass, and dead fuel mass in tallgrass prairie revealed strong

relationships between fuel bed parameters and soil moisture, expressed as fraction of available water capacity (FAW). LFMC exhibited a nonlinear, threshold-type relationship with FAW, with LFMC being insensitive to FAW at FAW levels above 0.56 and positively related to FAW below that threshold. In addition, this study provides a first step toward understanding the causal mechanism of live to dead fuel transition in the growing season in relation to FAW. Live to dead fuel transitions occurred around a FAW value of 0.34, with the rate of transition increasing approximately linearly as FAW dropped below that threshold. Estimating LFMC and transferring live fuels to dead based on observed FAW could contribute to better dynamic representations of fuel bed parameters in fire danger models. Improved fire danger ratings could enhance wildfire preparedness and response, which could help reduce the devastating impacts of wildfire on property and lives.

In the third study, we evaluated the potential of an existing forage model to see if we can simulate live mass and soil moisture using the previously calibrated plant parameters from the literature. The results indicated that improved plant and grazing parameters will be needed in order for the CROPGRO perennial forage model to be useful for near time forecasting of forage production in rangeland. The next step to enhance this simulation model would be calibrating the model with the data from 2012-2013 and then using additional site-years of data to validate the predictions of potential forage production for the growing season. The *B. brizantha* version of CROPGRO

perennial forage model, although adapted for little bluestem, did not accurately simulate live mass for 2012 and 2013. The severe and uncertainties about consumption rates and selective grazing influenced by the patch burn management could have complicated in live mass estimation. Though the CROPGRO perennial forage model was useful in simulating forage production in study sites in South America, the model requires improved parameter estimates to accurately simulate forage production in tallgrass prairie in Southern Great Plains of the United States. In contrast, the results from simulation of soil moisture suggest that the CROPGRO perennial forage model was useful for soil moisture prediction.

APPENDICES

CHAPTER II

Appendix A:

This appendix provides the connection weights to determine the importance of variables of interest as described in (Gevrey et al., 2003). This method involved the neural network with eight input variables, 15 hidden neurons and one output neuron with the connection weights as shown below,

	Weights (AGB)							
Output		CH	NDVI	460 nm	560 nm	660 nm	830 nm	1650 nm	Output
Hidden 1	-0.46	-1.45	-0.94	0.99	0.69	0.78	-1.14	-1.12	0.93
Hidden 2	-0.17	0.01	0.18	0.19	0.77	1.34	-0.09	-2.04	2
Hidden 3	-0.24	1.33	1.06	0.37	0.39	0.41	1.12	-0.14	-1.78
Hidden 4	-0.58	-0.82	0.56	-0.25	-0.29	0.053	-0.35	0.11	2.39
Hidden 5	-1.32	0.4	0.51	-0.45	1.74	-1.04	0.87	-0.75	1.81
Hidden 6	-0.22	-1.15	-0.7	0.33	-0.19	0.96	-0.20	-0.07	-1.43
Hidden 7	-0.04	1.3	-0.3	0.86	-0.002	-2.24	-0.70	1.23	1.33
Hidden 8	-4.35	0.44	-0.67	0.25	-0.32	0.81	-1.12	0.14	0.7
Hidden 9	0.34	-0.51	-0.81	-1.73	0.96	0.67	0.13	1.04	1.74
Hidden 10	-2.82	0.06	1.71	0.006	0.78	-0.75	1.07	-0.76	-0.9
Hidden 11	-0.98	0.56	0.51	-1.37	1.33	0.92	-0.29	0.27	-2.04
Hidden 12	-0.39	-1.04	-0.68	-0.69	-1.41	-0.54	-1.62	2.12	-1.56
Hidden 13	-0.56	0.74	0.59	0.05	-1.65	0.60	0.77	1.38	1.62
Hidden 14	-0.52	-1.02	0.07	0.3	0.19	-1.62	-0.44	-0.27	-1.07
Hidden 15	2.42	0.65	1.19	-0.72	0.82	-0.41	-0.13	1.33	1.07

	Weights (FMC)								
	DOY	CH	NDVI	460 nm	560 nm	660 nm	830 nm	1650nm	Output
Hidden 1	-0.54	-1.21	-0.95	1.41	0.48	-0.59	-0.91	-0.42	-1.88
Hidden 2	0.08	0.96	0.67	-1.03	0.22	1.13	0.68	-1.17	-1.82
Hidden 3	-0.39	-0.13	0.08	-0.91	-1.3	-0.05	0.09	-1.01	-1.10
Hidden 4	0.53	0.86	-0.39	1.95	-0.20	0.55	0.84	-0.38	-1.56
Hidden 5	0.71	1.01	0.53	0.40	2.24	-0.22	0.18	-1.37	1.38
Hidden 6	-0.73	1.04	-0.6	0.25	0.62	-1.0	-0.90	-0.14	-1.09
Hidden 7	0.27	-0.45	-0.38	-0.16	0.75	-0.06	-0.21	1.4	-1.94
Hidden 8	0.83	0.42	0.87	1.05	0.56	-1.24	-0.21	-0.11	-2.06
Hidden 9	0.63	-1.05	0.72	-1.39	-0.43	0.25	-1.30	0.96	-1.5
Hidden 10	1.93	-0.07	0.22	-0.63	-0.55	0.75	-0.39	-0.06	2.44
Hidden 11	1.61	1.29	-1.18	0.07	-0.43	1.37	0.41	-1.70	-0.95
Hidden 12	0.42	0.58	0.35	0.64	-0.02	-0.52	-1.32	0.87	1.40
Hidden 13	3.73	-0.03	1.18	0.45	0.34	-0.21	-1.35	0.06	1.02
Hidden 14	-2.37	-0.12	0.18	1.01	-0.67	0.19	-0.25	-0.47	1.63
Hidden 15	-1.12	-1.36	-1.11	1.04	-0.077	1.27	-0.97	-1.04	1.08

In addition, ANN provides bias parameters which are enumerated as follow.

bias	AGB	FMC
Hidden 1	-0.44	-0.53
Hidden 2	0.90	1.12
Hidden 3	0.24	-0.15
Hidden 4	-0.20	0.41
Hidden 5	0.25	1.39
Hidden 6	-0.12	0.05
Hidden 7	-0.09	-0.45
Hidden 8	0.97	0.66
Hidden 9	0.06	-0.40
Hidden 10	0.19	1.06
Hidden 11	0.79	2.07
Hidden 12	-0.01	-0.77
Hidden 13	0.30	-0.69
Hidden 14	-0.07	-0.10
Hidden 15	0.03	0.19
Output neuron	-0.10	0.28

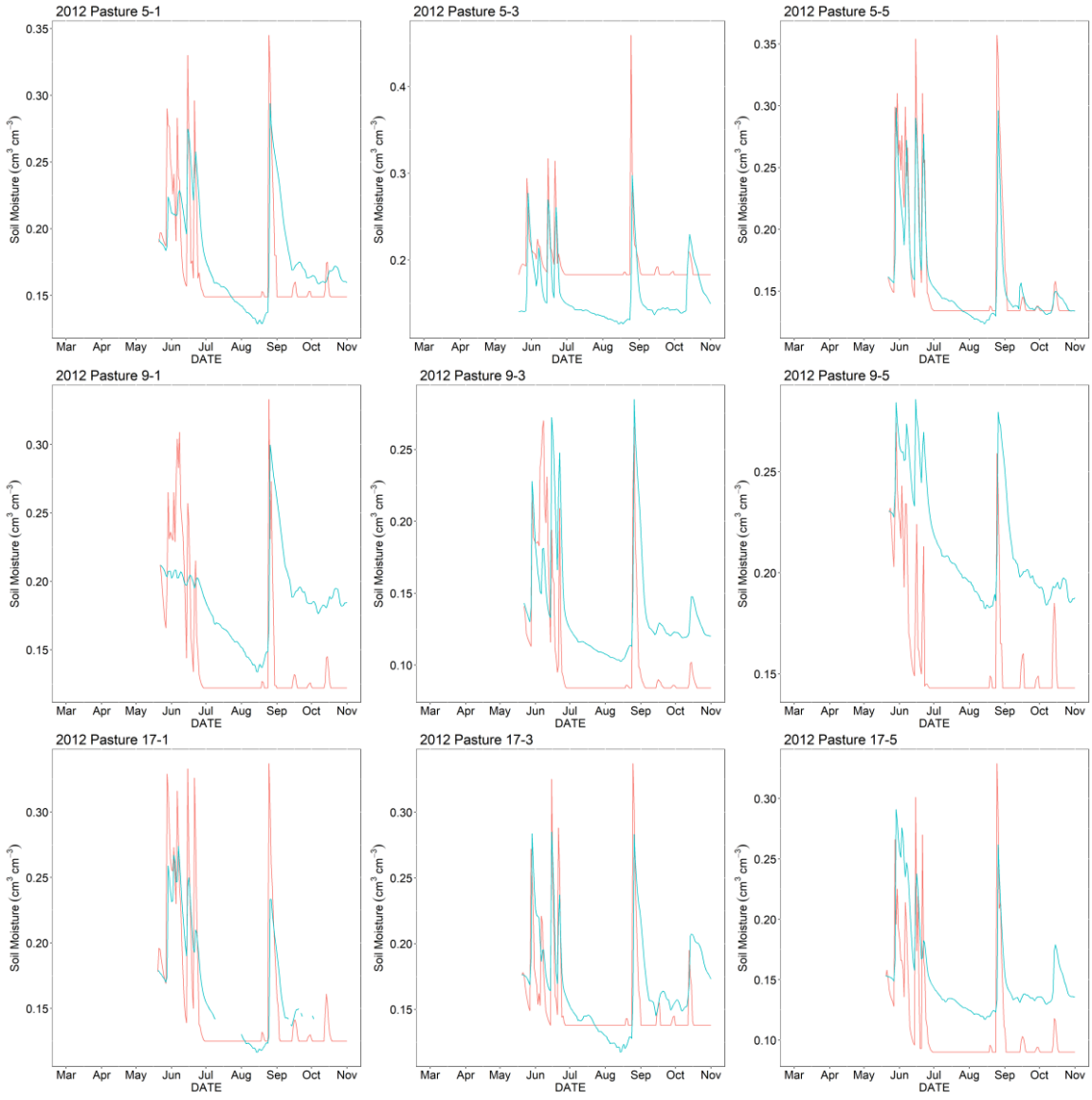

Fig. 1: Simulated and observed soil moisture for year 2012 at the tallgrass prairie at 10-20 cm depth in Stillwater, Oklahoma. The red line represents the simulated soil moisture whereas blue color represents the measured soil moisture

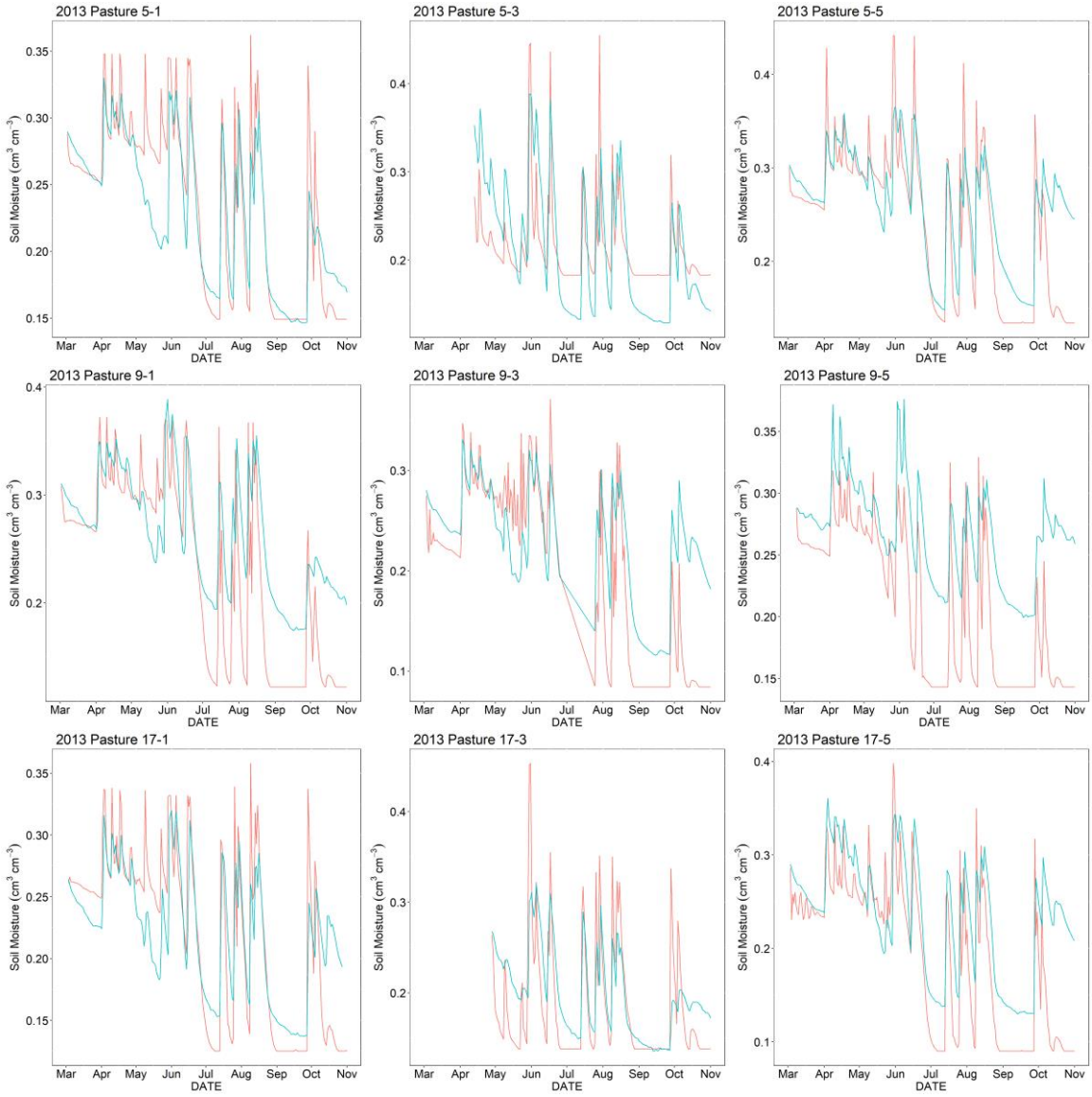

Fig. 2: Simulated and observed soil moisture for year 2013 at the tallgrass prairie for 10- 20 cm depth in Stillwater, Oklahoma. The red line represents the simulated soil moisture whereas blue color represents the measured soil moisture.

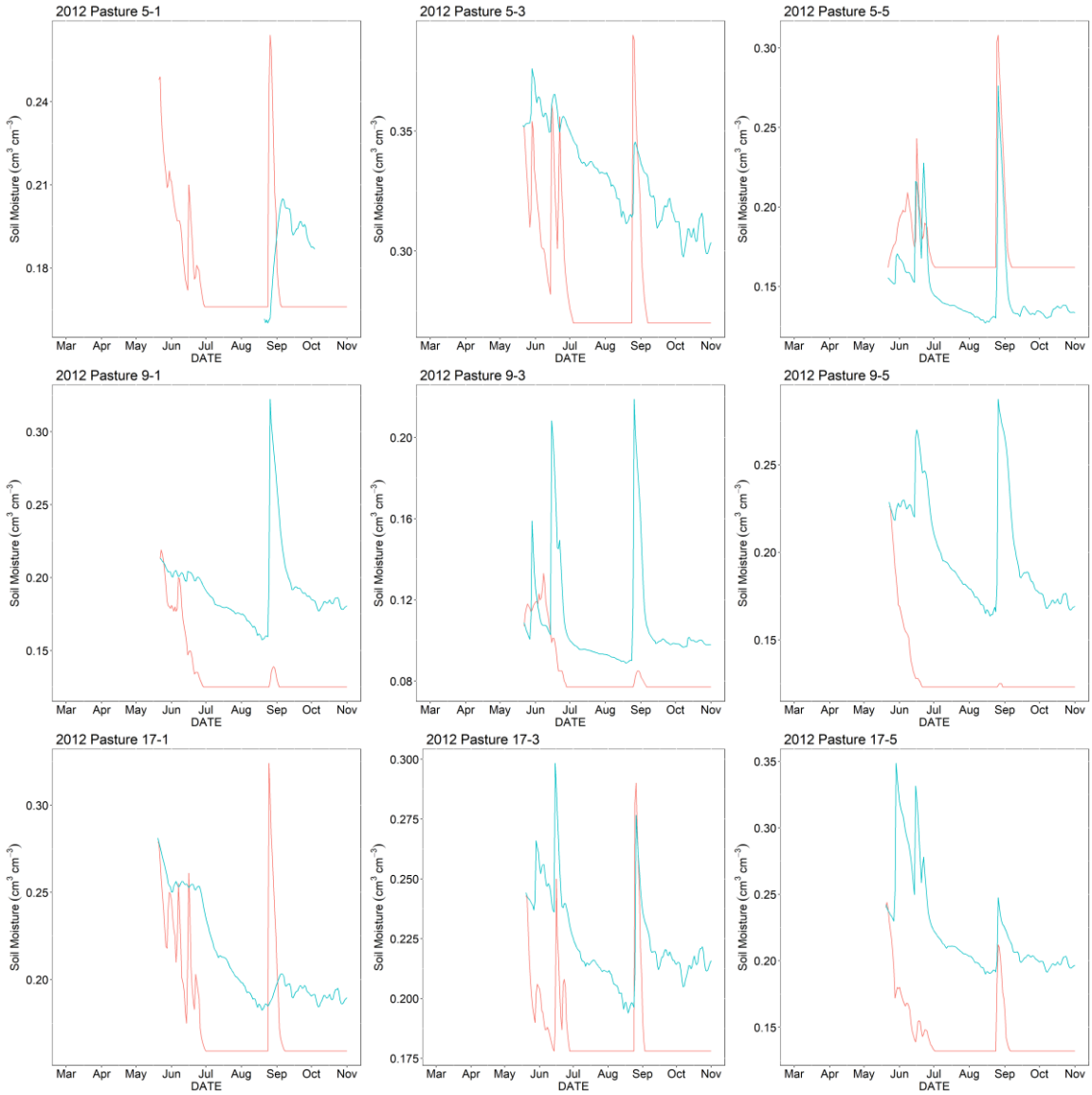

Fig. 3: Simulated and observed soil moisture for year 2012 at the tallgrass prairie for 20–50 cm depth in Stillwater, Oklahoma. The red line represents the simulated soil moisture whereas blue color represents the measured soil moisture.

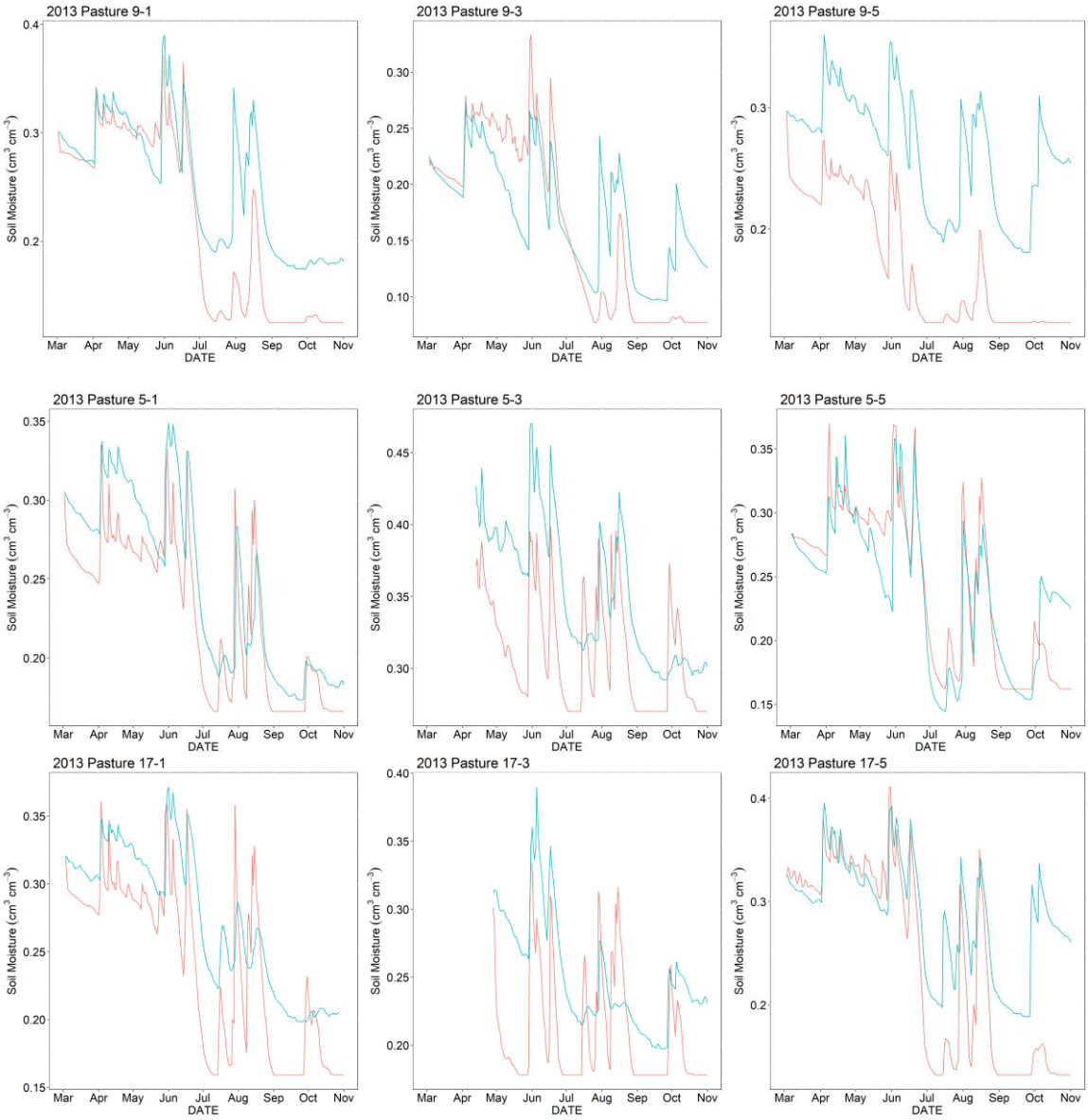

Fig. 4: Simulated and observed soil moisture for year 2013 at the tallgrass prairie for 20–50 cm depth in Stillwater, Oklahoma. The red line represents the simulated soil moisture whereas blue color represents the measured soil moisture

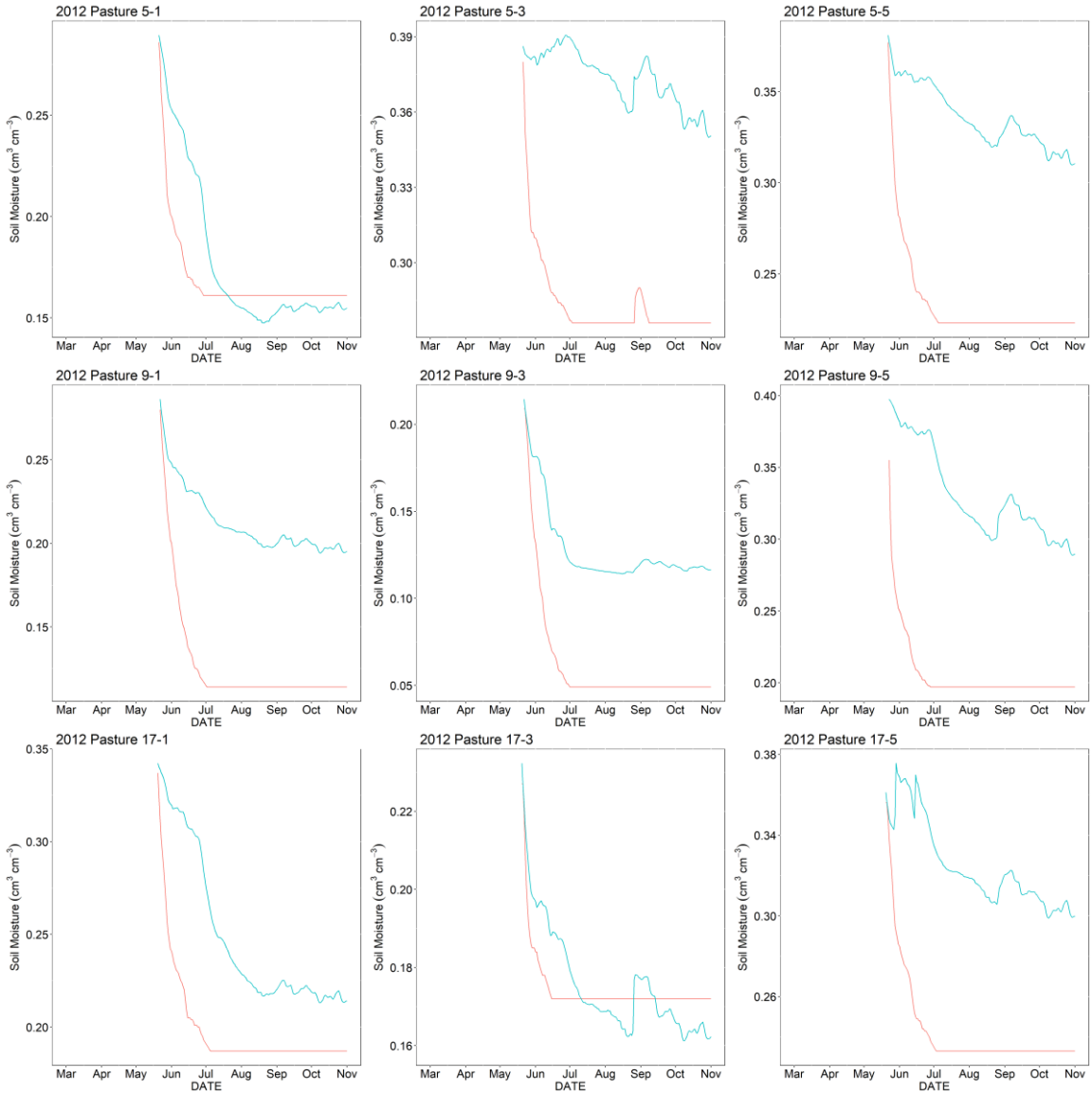

Fig. 5: Simulated and observed soil moisture for year 2012 at the tallgrass prairie for > 50 cm depth in Stillwater, Oklahoma. The red line represents the simulated soil moisture whereas blue color represents the measured soil moisture

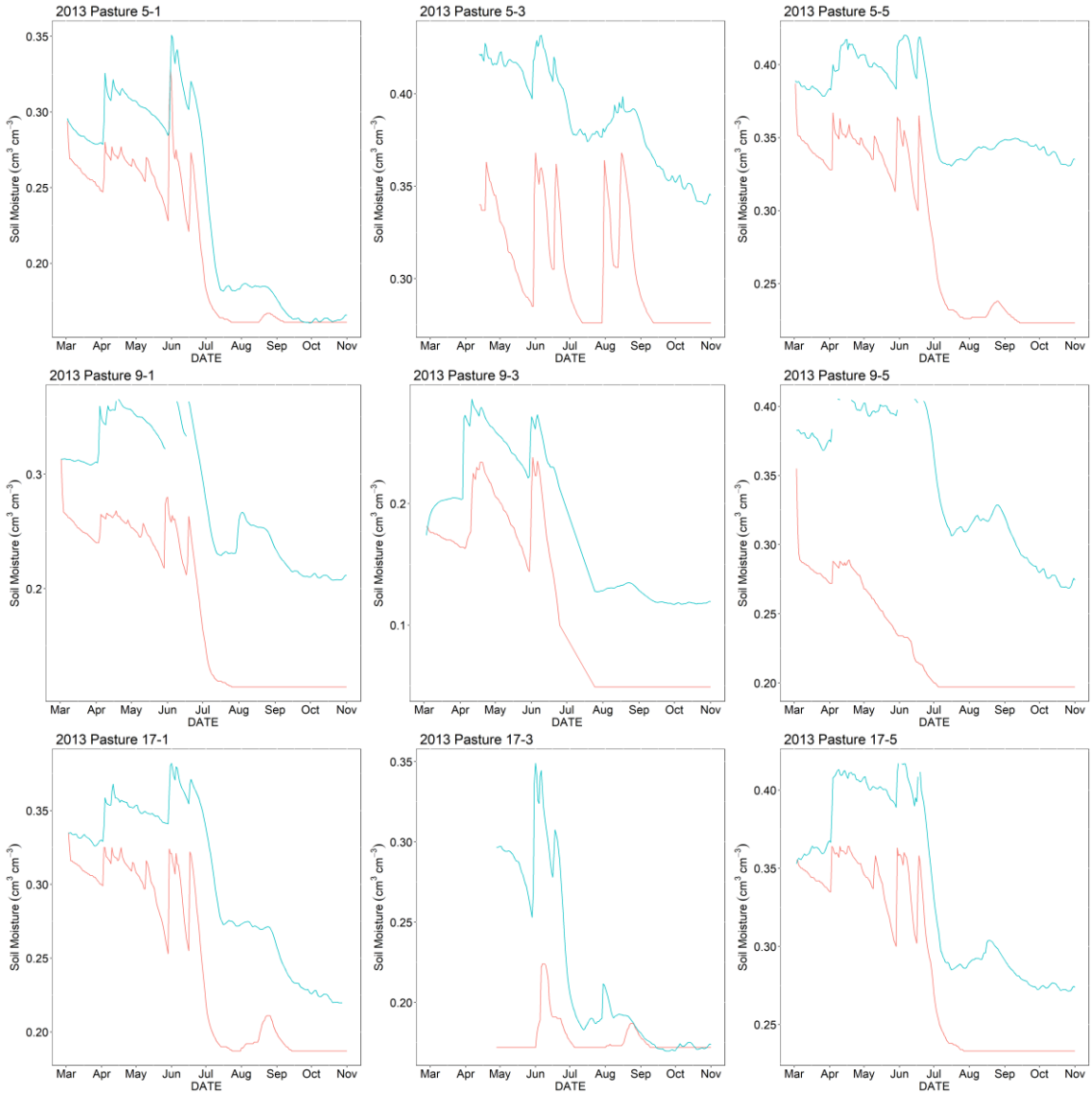

Fig. 6: Simulated and observed soil moisture for year 2013 at the tallgrass prairie for > 50 cm depth in Stillwater, Oklahoma. The red line represents the simulated soil moisture whereas blue color represents the measured soil moisture

VITA

SONISA SHARMA

Candidate for the Degree of

Doctor of Philosophy

Thesis: SOIL MOISTURE AND VEGETATION DYNAMICS IN SOUTHERN GREAT PLAINS GRASSLANDS

Major Field: Soil Science

Biographical:

Education:

Completed the requirements for the Doctor of Philosophy in Soil Science at Oklahoma State University, Stillwater, Oklahoma in July, 2017.

Completed the requirements for the Master of Science in Natural Resources at University of Nebraska-Lincoln, Lincoln, Nebraska in May, 2013.

Completed the requirements for the Bachelor of Science in Horticulture at Institute of Agriculture and Animal Sciences, Tribhuwan University, Nepal , August 2008.

Experience:

Graduate Research Assistant, Ph.D. Department of Plant and Soil Sciences, Oklahoma State University, Stillwater, OK. Supervisor: Dr. Tyson Ochsner. 2013-2017.
Graduate Research Assistant, M.S. School of Natural Resources, University of Nebraska-Lincoln, NE. Supervisor: Dr. Ayse Kilic. 2010-2013.
Program Officer, Ministry of Environment, Science and Technology, Government of Nepal, Lalitpur, Nepal. 2008-2009.

Professional Memberships:

Soil Science Society of America, Association of American Geographers, American Geophysical Union, Member, Soil and Water Conservation Society, Nepal Youth Red Cross Circle.